UNIVERSITY OF PARDUBICE
FACULTY OF CHEMICAL TECHNOLOGY

DIPLOMA THESIS

2018 Niloufar Rashedi Banafshehvaragh

University of Pardubice

Faculty of chemical technology

3D bioprinting using hydrogel and synthetic fillers

Niloufar Rashedi Banafshehvaragh

Diploma thesis

2018

Univerzita Pardubice
Fakulta chemicko-technologická
Akademický rok: **2017/2018**

ZADÁNÍ DIPLOMOVÉ PRÁCE
(PROJEKTU, UMĚLECKÉHO DÍLA, UMĚLECKÉHO VÝKONU)

Jméno a příjmení:	**Niloufar Rashedi Banafshehvaragh**
Osobní číslo:	**C16597**
Studijní program:	**N3441 Polygrafie**
Studijní obor:	**Polygrafie**
Název tématu:	**3D bioprinting using hydrogel and synthetic fillers**
Zadávající katedra:	**Katedra polygrafie a fotofyziky**

V Pardubicích dne 11. května 2018

Rozsah grafických práce:	**dle potřeby**
Rozsah pracovní zprávy:	
Forma zpracovaní diplomové práce:	**tištěná/elektronická**
Seznam odborné literatury:	**Podle pokynů vedoucího diplomové práce**

Vedoucí diplomové práce:	**doc. Ing. Petr Němec, Ph.D.** Katedra polygrafie a fotofyziky

Datum zadání diplomové práce:	19. prosince 2017
Datum odevzdání diplomové práce:	11. května 2018

I hereby declare that I have written this master thesis on my own. All the literary sources and the information used are listed in the bibliography.

I was familiar with the fact that rights and obligations arising from the Act No. 121/2000 Coll., the Copyright Act, apply to my thesis, especially the fact that the University of Pardubice has the right to enter into a license agreement for use of the paper as a school work pursuant to § 60, Section 1 of the Copyright Act, and the fact that should this thesis be used by me or should a license be granted for the use to another entity, the University of Pardubice is authorized to claim a reasonable fee to cover the costs incurred during the making of the paper, up to the real amount thereof.

I agree with the reference-only disclosure of my thesis in the University Library.

10th May 2018 in Pardubice

Niloufar Rashedi Banafshehvaragh

At this point, I would like to express my gratitude to my German supervisors Prof. Aldo R. Boccaccini and Dr. Rainer Detsch. This work would not be ever completed without their constant encouragement, and assistance in numerous ways. I also acknowledge the contributions, advice and suggestions of Dr.-Ing. Samira Tansaz, and I am very grateful to my Czech supervisor Petr Němec as well.

Additionally, I would like to thank the Institute for Biomaterials at the Department of Materials Science and Engineering, Friedrich-Alexander University Erlangen-Nürnberg for its outstanding academic support.

NÁZEV PRÁCE

3D biotisk pomocí hydrogelu a syntetických plniv

ANOTACE

Cílem tohoto výzkumu je porovnání čistého polykaprolaktonu (PCL) a kombinace směsi polykaprolaktonu a polyethylenglykolu (PCL-PEG) spolu s alginát dialdehydovým želatinovým hydrogelem (ADA-GEL) pro výrobu 3D skafolů biotiskem.

KLÍČOVÁ SLOVA

3D biotisk; přídavná výrobní technika; biologická výroba; tkáňová technika; polykaprolakton; alginát dialdehydová želatina; hydrogely

TITLE

3D bioprinting of cell-loaded constructs using hydrogel and synthetic fillers

ANNOTATION

The aim of this research is to make a comparison between pure polycaprolactone (PCL) and a combination of polycaprolactone and polyethylene glycol (PCL-PEG) blend together with alginate dialdehyde gelatin hydrogel (ADA-GEL) to fabricate 3D scaffolds with sequential bioprinting process.

KEYWORDS

3D bioprinting; additive manufacturing technique; biofabrication; tissue engineering; polycaprolactone; alginate dialdehyde gelatin; hydrogels

CONTENT

LIST OF FIGURES

LIST OF TABLES

LIST OF ABREVIATIONS

UV	Ultraviolet
AMT	Additive manufacturing technique
PCL	Polycaprolactone
PEG	polyethylene glycol
ADA-GEL	Alginate dialdehyde gelatin hydrogel
SEM	Scanning electron microscope
FDM	Fused deposition modelling
CT	Computed tomography
MRI	Magnetic resonance imaging
STL	Stereolithography
LIFT	Laser-induced forward transfer
ROP	Ring-opening polymerization
ε-CL	ε-caprolactone
PAAm	Polyacrylamide
PCMs	phase change materials
SSPCMs	Shape stabilized phase change materials
PEGDA	Poly(ethylene glycol) diacrylate
RGD	Arginine–glycine–aspartic acid
GAGs	Glycosaminoglycans
ECM	Extra cellular matrix
HA	Hyaluronic acid
MA	Maleimide modified
EDTA	Ethylene diamine tetra acetic acid
DPBS	Dulbecco's phosphate buffered saline

0. INTRODUCTION

3D bioprinting, defined as an emerging versatile technology which concerns regeneration of medical non-biological implants by 3D printing, is considered as a recently developed technique which is increasingly used to design and manufacture living tissues and organs that can be implanted into human body. By the help of this breakthrough, growing demand for replacement of tissues and organs can be excellently alleviated, while it has opened a promising ground for research models and appropriate replacement of human body organs and tissues with 3D printed tissues already implanted into patients in certain experimental cases [1].

It is worth mentioning that historical development of 3D printing owes much to Charles Hull, who patented in 1986 a method of printing ultraviolet (UV)-curable materials on top of each other in a layer-by-layer fashion called stereolithography. His technique served as the basis for constructing further 3D printing systems (also called rapid prototyping or additive manufacturing in general). Broadly speaking, 3D printing involves the sequential deposition of any material capable of solidification in a cross-sectional pattern for the building-up of a three-dimensional object [2].

Technology of biopritning can be categorized according to the fact, whether the final printed object is 2D or 3D. Example of a 2D bioprinted object can be a 2D pattern comprised of cells on a surface, by incorporating a hydrogel or other cell-friendly biomaterial. The limitation of 2D cell patterns proliferative capacity and are sensitive and fragile in in vitro environments, thus requiring customized, supportive environments that mimic their in vivo environments to maximize cell viability and function [2]. In contrast, 3D cellularized structures, fabricated in a drop by drop manner, have replaced previous rigid scaffold seeding approaches and provide cellular environments more like those in the body [2].

Nowadays, 3D printers are widely used to prototype, design and manufacture different devices or objects. Among other applications, they have growing capacity to be utilized in different areas of regenerative medicine, drug delivery and testing, disease modelling and tissue or organ engineering. According to Atala and Shafiee [1] end-product of this printing method can generally be divided to nonbiologic 3D printed and bioprinted. The former consists of methods to prototype and model implants for different purposes without biologically active material and the later regards cell and tissue printing, in its broad sense, to replace those missing or damaged

in the human body. Current researches and experiments help us list applied techniques and materials. Most of these applications belong to the previous two decades and range from surgical planning to 3D models, consisting wide range of applications such as liver replicas and intermediate splints and more recent researches which explore this technology to fabricate different tissues such as blood vessels and cardiac patches [1].

As the title of thesis indicates, the concentration of this research will be on Additive Manufacturing Technique (AMT) in 3D bioprinting, namely biofabrication in general, enabling rapid construction of 3D structures with complex geometries using a diverse range of synthetic and natural materials [2]. This technique is a state-of-art development which makes possible printing of biocompatible materials along with supporting elements and cells into a complex 3D living tissue. Though basically similar to nonbiologic 3D printing, 3D bioprinting requires more careful attention to a set of parameters which affect the final product. Choice of material, cell types, growth/differentiation factor, and technological challenges must be attentively considered [2].

Major pillar of AMT is construction of a biocompatible network of synthetic or natural polymers, sometimes mixture of both, called scaffold or support structure, which serves as an extracellular matrix mimicry for cells to engineer tissue grafts of different variety [3,4]. Typically-used material for the support structure is non-adhesive cell-loaded hydrogel, which is a class of choice for cell immobilization and helps the printed construct maintain its shape until post-printing formation. As the division of printing modalities indicates [2], extrusion-based deposition of AMT relies heavily on mechanical and temporal polymer or/and hydrogel properties being printed. The way that they are printed is extrusion through a (set of) syringe(s), driven by computer-controlled pneumatic pressure or mechanical pistons. Mechanical and temporal properties ensure facilitated extrusion of materials, which is affected by softness and fluidity of the material, as they must run through a small-diameter syringe tip or nozzle, while being able to support themselves after deposition as a scaffold. These properties can be strengthened and justified by addition of synthetic fillers to the basic hydrogel. Melt-curable polymers or thermoplastic materials in general, such as PCL, which can be deformed after being heated and printed afterwards at relatively high resolution followed by cooling down to a solid material, are among the suitable fillers which can accompany basic hydrogel and compensate its lack of mechanical integrity [2].

However, PCL can also be mixed with other synthetic polymers, such as polyethylene glycol and bioactive glasses, which is the main interest of this research. Studying the properties of extruded materials leads to better understanding of the whole process, matching these properties with those required for cell culturing, and opens up the ground for further researches with specific objective in every singular application.

0.1. Purpose

The aim of this research is to make a comparison between pure PCL and a combination of polycaprolactone and polyethylene glycol (PCL-PEG) blend together with the basic material alginate dialdehyde gelatin hydrogel (ADA-GEL) to fabricate 3D scaffolds in sequential bioprinting process. Chemical properties, miscibility and wetting behavior of all the materials used will be evaluated. Scaffolds will be characterized according to porosity, pore size, mechanical stability and strut width. By the help of scanning electron microscope (SEM) incubated scaffolds will be compared with those non-incubated. This way, the effect of thermoplastic materials in combination with soft hydrogel to strengthen the rigidity of bioprinted scaffolds will be studied.

0.2. Research background

The issue of optimization of hydrogels considering mechanical properties and shape stability can be tackled by combining different additives, such as hot-melt extruded thermoplastics together with cell loaded hydrogels in a sequential printing process. The result will be fabricated 3D constructs which are mechanically supported by the thermoplastic structure and biologically functionalized by the hydrogel phase [5]. Different approaches to treat this issue have been reported.

One approach is introduced in an article by Duan et al. [6] which concentrates on infiltrating cell-loaded hydrogel in pre-fabricated 3D constructs, such as infiltrating of nanofibers fabricated by electrospinning. Electrospinning, according to Wang and Kumar [7], is a viable technique to produce nanofibers, i.e. spinning fibers with the help of electrostatic forces, capable of producing fibers in the submicron range. Visser et al. [8] reported fabrication of highly porous 3D polycaprolactone microfiber support construct using melt electrospinning writing. It was infiltrated in the next step with gelatin methacrylamide loaded with human

chondrocytes. Hutmacher et al. [9] established dispense plotting of PCL using fused deposition modelling (FDM), allowing the design and fabrication of highly reproducible bioresorbable 3D scaffolds with a fully interconnected pore network. Other approaches consider as well coating PCL scaffolds for cell response improvement [10] which deals with improvement of surface properties of PCL. However, other research activities have tried to modify the bulk material instead of just changing surface properties. Modification of basic extruded material by adding PCL and PEG can be found in researches by Hoque et al. [11] and Jiang et al. [12] and using PCL-PEG blends in Patrício et al. [13]. Application of PCL as a thermoplastic hard phase and a hydrogel with immobilized cells to create mechanically enhanced 3D structures by sequential bioprinting technique has been the research interest of Schuurman et al. [14]. Sequential bioprinting technique is a layer by layer approach which enables the freedom for designing constructs with different materials and cell types in pre-defined positions, which are then fabricated in a one-step process. Regarding seeding efficiency and cell distribution, it is superior to the cell-seeding method of PCL scaffold [15].

1. THEORETICAL FRAMEWORK

1.1. Medical application of 3D printing

As already mentioned in the introduction, printed products of medical application of 3D printing can be divided to two broad categories of nonbiologic and bioprinted (3D printing of biological object). Based on this division, materials that are used in this technology can be categorized and further identified. Analogous to conventional printing, Medical application of 3D printing involves three main steps as well to print the end-product: **Pre-printing, (bio)printing, and post-bioprinting**. The later only applies to biologic 3D printing, where cell culture and formation plays a key role in the whole process. Considering these broad divisions regarding process and end-products, following parts will discuss in detail the process and materials involved in medical application of 3D printing.

1.2. Pre-printing

In case of **non-biological** implants such as ear prostheses or mandibular replacement, one can reproduce the required organ using 3D printer with more precise and personalized approach, compatible with the patient's own specifications. In these cases, 3D imaging software helps

model the required body as pre-press process. Historically, Charles hull invented 3D lithography in 1989, opening up a new realm in industry to produce complex objects not possible otherwise [16]. In case of biological objects, medical imaging helps provide information on 3D structure and function at the cellular, tissue, organ and organism levels.

The two most common imaging technologies for medical application of 3D printing are Computed tomography (CT) and magnetic resonance imaging (MRI). The role of any of these imaging methods is to achieve segmental 2D images for the layer-by-layer fabrication process after medical imaging and tomographic reconstruction is performed. Detailed explanation of using these methods in living donor liver transplantation can be found in a research by Zein et al. [17]. Digital preparation and 3D representation of the target object, either organ or tissue, in form of stereolithography files (STL files), which will be later transferred to the printer, plays the next key role after considering the appropriate printing technique and requirements of the end-product. Moreover, mathematical models are recent efforts to collect and digitize the complex tomographic and architectural information for tissues [18].

1.3. Printing technologies

As comparable to any conventional printing technology, medical application of 3D printing consists of a printing machine, ink (bioink) and substrate, i.e. material on which the ink will be deposited. Printing technology can be divided to three main types: inkjet-like devices, laser-assisted, and extrusion devices [19]. Figure 1 provides a brief overview of common printing technologies for medical applications. In the following parts, a closer look at each of these three types of printers will be presented.

1.3.1. Inkjet-like printing

Inkjet printers have two traditional categories: continuous and drop-on-demand [2]. First category inkjet printers run with higher speed, while being able to print on large-scale areas. In comparison, drop-on-demand type of inkjet printers are more efficient from economic point of view and operate more precisely [20]. The category of drop-on-demand printers can also be divided to thermal and piezoelectric inkjet printers. In piezoelectric drop-on-demand printers, a voltage pulse is applied to change the size and shape of the piezoelectric material and, consequently, a droplet of ink is produced by pressure on the ink reservoir caused by the

piezoelectric material [2]. Adjusting the shape and size of the droplet can be adjusted by tuning the applied voltage to the piezoelectric material. In case of thermal printers, a bubble of ink is made by a heater out of the reservoir, which later will be ejected from the nozzle of the device [2].

When it comes to medical application of 3D printing, drop-on-demand inkjet is mostly

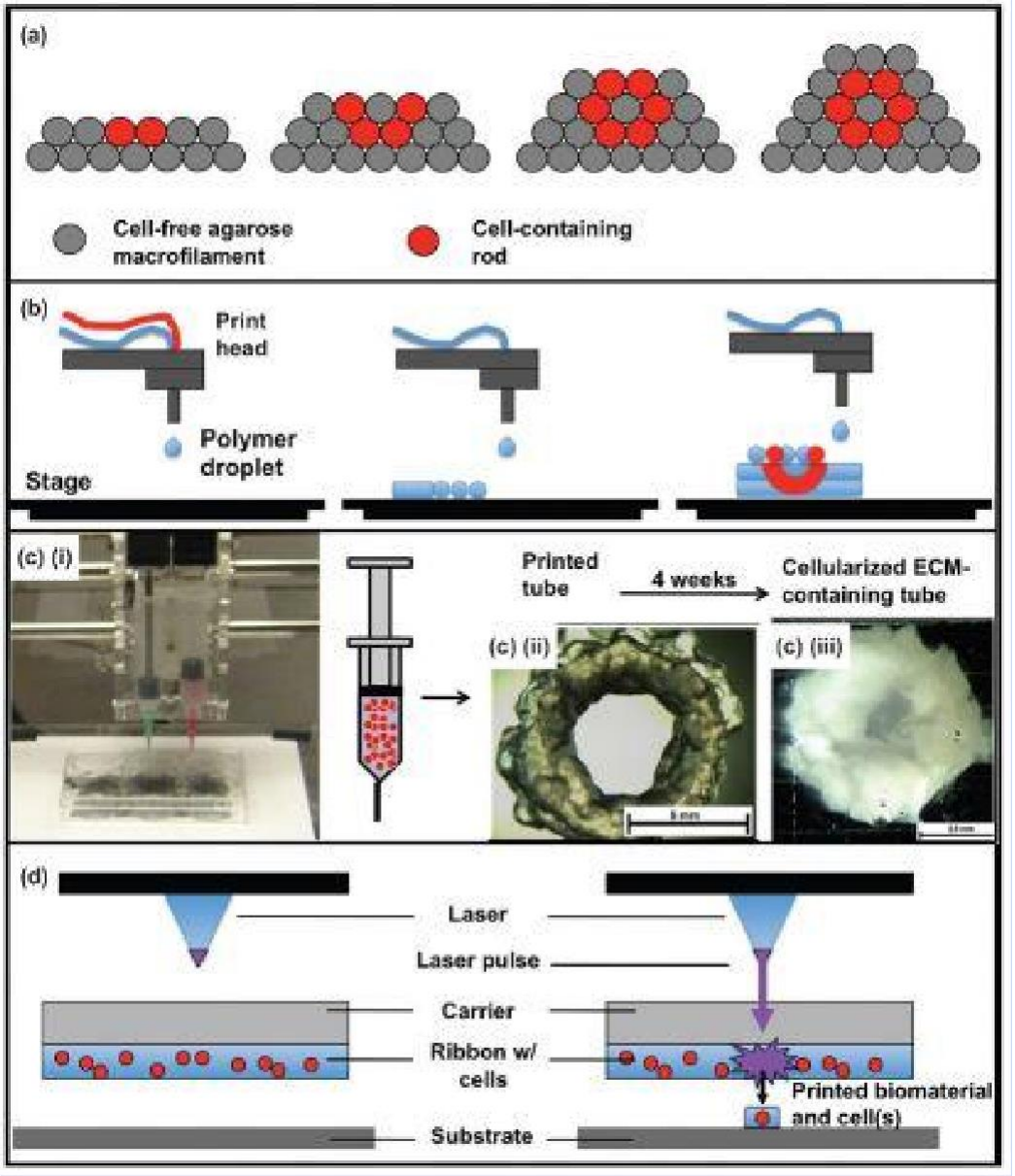

Figure 1 Printing technologies for bioprinting applications. (a) Scaffold-free printing; (b) inkjet droplet printing; (c) extrusion printing; and (d) laser-induced forward transfer (LIFT)-based printing. (c) (i) A syringe-based extrusion printer; (c) (ii) Extruded cell-hydrogel tubes that (c) (iii) mature over time into cellularized ECM-containing tubes [2]

preferred. Its main application can be found in cell patterning, i.e. drop by drop printing of cells to fabricate cellularized structures, as an example [21]. Configuration of these printers consists of a cartridge similar to that used in traditional inkjet printing such that cells and biomaterial components can be loaded into individual cartridges for computer-controlled deposition based delivery system mounted on an XYZ plotting device [1]. Creating muscle patches using droplet form which includes collagen-encapsulated smooth muscle cells is an example of implementing drop-on-demand inkjet printing [22]. Another example is the use of alginate and fibrin gel droplets for creating structures such as cellular fiber and multilayered cell sheets [23]. Using inkjet printing for skin printing to aid wound healing has also been reported by Skardal et al. [24].

Importance of polymerization and cross-linking chemistries has been clearly explained by Skardal et al. [24]. When it comes to 3D fabrication, the drop-by-drop approach must rely on being able to quickly polymerize or stabilize the printed material in place, so that subsequent droplets can be added to the growing structure. Various cross-linking chemistries innate to materials used can determine the polymerization rates of the printed materials are an essential consideration for successful printing. However, the need for a fast-gelling material places a limitation on the types of materials that can successfully be applied in this manner. Plus, as the printable droplets are typically small volumes, scaling up to fabricate a large organ structure might be difficult. On the other hand, the small droplet volumes support high-resolution printing of intricate structures.

1.3.2 Laser-assisted printing

This approach is a recently introduced method adopted from other fields and has been reported in some researches about bioprinting. As opposed to Inkjet technology, laser-assisted printing lacks nozzles in device configuration, which is an advantage to this technology, as it avoids common problems such as clogging. As stated by Bohandy et al. [25] and Barron et al. [26], this technology deals with Laser-induced forward transfer (LIFT)-based bioprinting, which has been initially developed for high-resolution metal patterning in computer chip fabrication. More recently this technology has been applied to create micro-pattern peptides, DNA, and cells [2].

Configuration of a LIFT device consists of a laser beam, pulsing at time lengths that have been set in advance, and a ribbon which functions as material donor where printable materials are loaded. This ribbon is supported by a transport layer which must be able to absorb the laser

energy and later transfer it to the ribbon. Example of this transport layer can be gold or titanium. As the laser sends pulses on the ribbon, the laser energy will be focused and it leads to a small, though high pressure, bubble which enforces a droplet of the donor material to release onto the substrate. Patterning the given material can be achieved by either moving the substrate or the laser in relation to the ribbon [27].

Having in mind this basic function of LIFT, one should note that when it comes to LIFT-based bioprinting, the difference is that the ribbon is comprised of biopolymers or proteins, containing cell within itself. In this case, the laser pulse-driven ribbon droplets contain cells, which are then deposited in a pattern on the substrate to create cellular structures and patterns [2].

Among the capabilities and advantages of Laser-induced forward transfer method one can name increasing flexibility in the printing material, no negative effect of cell viability as an important factor in bioprinting, and the ability to print nearly a single cell per droplet [28]. In general, one can position this technology with much potential in the future.

According to Guillemot et al. [28], there are a number of variables, which lead to high resolution of LIFT. Laser itself, the material properties of the printable material, the relative hydrophilic/hydrophobic nature of the substrate material to the printable material, cell density, and the distance between the ribbon and the substrate. On the other hand, there are three notable challenges to be overcome regarding LIFT. Firstly, the high resolution and subsequently small printing volume per laser pulse requires fast gelation kinetics of the printable material and a fast-moving stage for fabrication. Secondly, preparation times of the ribbon in current LIFT methods, especially when containing cells and thus cell-friendly biomaterials, can be time consuming. Thirdly, to create structures of size, multiple ribbons are often employed, requiring reloading during the printing process.

1.3.3. Extrusion printing

Extrusion-based deposition of biomaterial is another approach for 3D bioprinting which is generally realized by a syringe-like device, accompanied by a pressure box. What mainly matters in this technology are the mechanical and temporal properties of the polymer materials being printed [2]. As already mentioned in the introduction, the way that hydrogel or polymer material are printed is extrusion through a (set of) syringe(s), driven by computer-controlled pneumatic pressure or mechanical pistons. Mechanical and temporal properties ensure

facilitated extrusion of materials, which is connected to their softness and fluidity, as they must run through the small diameter syringe tip or nozzle, while being able to support themselves after deposition into scaffold. These properties can be strengthened and justified by addition of synthetic fillers to the basic hydrogel. Melt-curable polymers, such as PCL, which can be deformed after being heated and printed afterwards at relatively high resolution followed by cooling down to a solid material, are among the suitable fillers which can accompany basic hydrogel and compensate its lack of mechanical integrity [2]. These materials are capable of building rather large and intricate structures, which mimics physiological structures. The main reason for cell seeding in the next stage, as opposed to two above-mentioned printing technologies where cells are included in the ink, is the presence of melt-cure polymers in the process, which will affect cell viability and negative modification if applied directly in the initial extruded material. Incorporation of hydrogel plays here the role of cell-friendly material to host cells at cell seeding stage. Among the challenges that this technology presents, is the time span required for gelation or crosslinking of hydrogel. Mistiming the deposition process can result in either a structure that collapses because cross-linking has not occurred quickly enough, or conversely, clogging of the bioprinting device as a result of polymerization that was too fast. However, numerous studies have implemented novel methods and cross-linking chemistries to control extruded materials spatially and temporally, which contain encapsulated cells for printing cell-loaded 3D support constructs [2].

1.3.4. Essential Considerations

According to Atala and Yoo [2] there are four general variables that must be considered attentively in order to successfully bioprint viable and functional tissue constructs:

I. **Cellular component** comprising the living portion of the construct, which can be comprised of one cell type, but more often than not requires a complex but elegant interplay between multiple cell types to achieve significant tissue function.

II. **Inclusion of supportive biomaterials**, generally in the form of proteins and polymers, that (a) facilitate the deposition method by mechanical means and (b) provide support and protection to the cells during and after the tissue construct fabrication process. These biomaterials can encompass the physical environment inside of which the cells will reside, as well as the biochemical signals cells need to function as they would in the body.

III. **Actual bioprinting or biofabrication device** itself and the associated method by which fabrication is performed, be it inkjet, extrusion printing, or another modality. The way that these first three variables are integrated plays the largest role in successful bioprinting.

IV. **Postfabrication** maintenance and maturation. This step often employs the use of bioreactors, which either condition the tissue constructs in some manner, priming them for their end application, or in some cases, the operation of the bioreactor is the end application such as in in vitro applications like toxicology screening.

1.4. Biomaterials and Bioinks

The terminology that will be used in this part will be briefly clarified. Biomaterial refers to a wide range of materials, including technologies that are considered as new phenomena, unthinkable even a decade ago. The category of these materials is still expanding as well as the classification of biomaterial types. The range of biomaterial encompasses stiff metal or ceramic implants, to cell supportive soft hydrogels or nanoparticles and quantum dots for drug delivery and imaging or even complex functioning medical devices such as left ventricular assist devices and artificial hearts [1].

However, when it comes to medical application of 3D printing, we can narrow down this wide category to two primary ones according to Skardal et al. [29]:

I. Curable polymers that result in mechanically robust (i.e., stiff or durable) materials that provide structure to printed constructs.

II. Soft biomaterials such as hydrogels, generally with a high content of water, inside of which cells are capable of residing.

In following sections an overview of these two categories along with relevant examples will be discussed.

1.4.1 Curable polymers; Case of PCL

Historically, the basic idea behind medical applications of 3D printing was fabricating metal and thermoplastic structures which employed melting and consequent curing. Incompatibility of melting and curing polymers with living cells such as proteins and cellular signaling molecules arises from the fact that in these processes high temperature, toxic organic solvents or cross-linking agents are actively involved. Having all these disadvantages in mind, there was

a strong advantage of polymers which supported their extensive implementation strongly: robust mechanical properties associated with such materials once cured [29].

One of the class of choice synthetic polymers, whose properties and advantages for medical applications of 3D printing were considered recently is PCL. PCL, as a polyester-based material, proves to be able to be biodegraded by the body and to have relatively low melting temperature of 60°C with hydrophobic character, which make it appropriate to be a structural scaffold printing component [29]. Its main challenge is lack of natural motifs that provide specific binding sites for cells that facilitate tissue integration. Due to this defect, PCL had better be combined with other functionalized materials or naturally derived materials, such as hydrogels, leading to an integrative approach to medical application of 3D printing.

Polystyrene is another example of melt-curable polymers. However, the high temperatures associated with reaching a flowing melt state that can be extruded has limited their applications beyond structural components [2].

General properties of PCL

PCL, firstly synthesized by the Carothers group in early 1930s, is a synthesized polymer, which is also biodegradable by many microbes in nature [30]. According to Atala and Yoo [2] advantageous properties of PCL can be listed as:

I. Good solubility (in acetone, 2-butanone, ethyl acetate, dimethylformamide and acetonitrile);
II. Low melting point (59–64 °C);
III. Glass transition temperature of −60 °C;
IV. Exceptional blend-compatibility to improve stress crack resistance and adhesion.

It is worth mentioning that crystalline nature of PCL enables easy formability at relatively low temperatures and is often used as an additive for resins to improve their processing characteristics and their end-use properties (e.g. impact resistance). These properties make this chemical appropriate for biomedical applications in such a way that recently it has been investigated as a scaffold for tissue repair via tissue engineering and guided bone regeneration membrane [31]. Before birth of the tissue engineering field, PCL was considered as a replacement material for metal devices used in medical implantations. Though it's weak mechanical properties prevented it from being used in high load bearing applications. This almost forgotten chemical came gradually into the scene during past decades [32].

Generally speaking, PCL bears some unique properties, such as controlled degradability, miscibility with other polymers, biocompatibility and potential to be made from monomers derived from renewable sources, which justifies its emerging popularity.

Regarding PCL application in 3D bioprinting, according to Hutmacher [33] the following characteristics are desirable for scaffold candidates which correspond to PCL characteristics:

I. Three-dimensional and highly porous structures with an interconnected pore network, for cell growth and flow transport of nutrients and metabolic waste;
II. Biocompatible and bioresorbable with a controllable degradation and resorption rate to match cell/tissue growth in vivo;
III. Suitable surface chemistry for cell attachment, proliferation and differentiation;
IV. Mechanical properties to match those of the tissues at the site of implantation.

PCL is an incredibly versatile bioresorbable polymer and by way of its superior rheological properties it can be used by almost any polymer processing technology to produce an enormous array of scaffolds [33].

Preparation of PCL

According to Labet and Thielemans [34], there are two common pathways to produce PCL. One of them is the polycondensation of a hydroxycarboxylic acid: 6-hydroxyhexanoic acid, and the other the ring-opening polymerization (ROP) of a lactone: ε-caprolactone (ε-CL) or radical ring-opening polymerization of 2-methylene-1-3-dioxepane. In either of these preparation pathways, monomers of 6-hydroxyhexanoic acid or ε-CL must be prepared first. These are by-products of oxidation of cyclohexanol to adipic acid by a number of microorganisms [35] as shown in Figure 2.

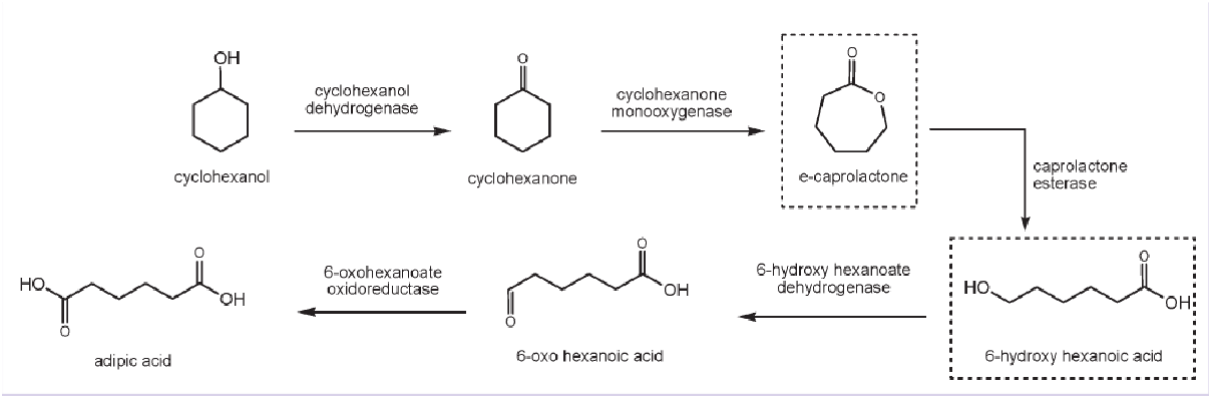

Figure 2 Oxidation of cyclohexanol to adipic acid adapted from Thomas et al. [35]

In the following sub-sections, polycondensation and ROP of PCL preparation will be discussed.

Polycondensation of a hydroxycarboxylic acid

In a paper by Braud et al. [36] PCL oligomers were synthesized by polycondensation of 6-hydroxy- hexanoic acid under vacuum, where the water produced during the reaction was removed. In this reaction no catalyst was used and it was complete in 6 hours at a temperature that was gradually increased from 80 to 150 °C.

In comparison to ROP, polycondensation gives a polymer with lower molecular weight but higher polydispersity. In practice, ROP is a preferred route to polycondensation.

Ring-opening Polymerization (ROP) of ε-CL

ε-CL is a cyclic ester, namely lactone, with a seven-membered ring as shown in Figure 3.

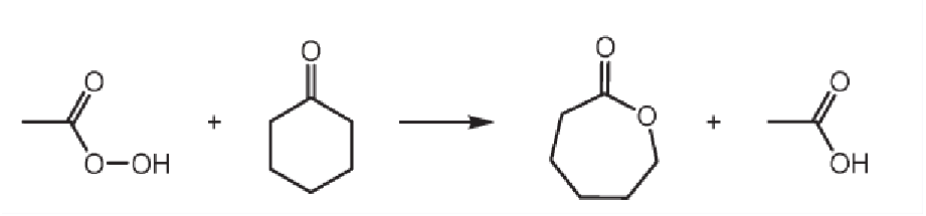

Figure 3 Production of ε -caprolactone from cyclohexanone [34]

PCL is catalyzed by stannous octoate and molecular weight of the polymer can be controlled by low molecular weight alcohols [31]. Depending on the catalyst, four main mechanisms exist for the ROP of a lactone, each resulting in different molecular weight, molecular weight distribution, end group composition and chemical structure of the copolymers [32].:

I. Anionic: involves the formation of an anionic species which attacks the carbonyl carbon of the monomer. The monomer is opened at the acyl–oxygen bond and the growing species is an alkoxide (Figure 4).

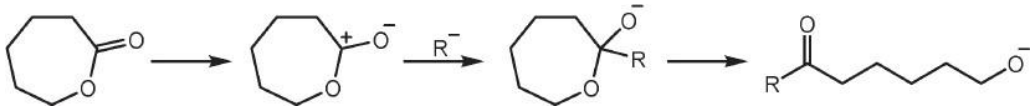

Figure 4 Mechanism of the initiation step for anionic ROP [37]

II. Cationic: involves the formation of a cationic species which is attacked by the carbonyl oxygen of the monomer through a bimolecular nucleophilic substitution (SN2) reaction (Figure 5).

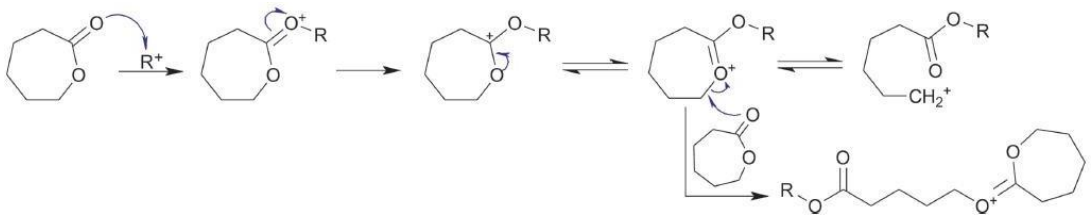

Figure 5 Mechanism of the initiation step for cationic ROP [38]

Ⅲ. Monomer-activated involves the activation of the monomer molecules by a catalyst, followed by the attack of the activated monomer onto the polymer chain end (Figure 6).

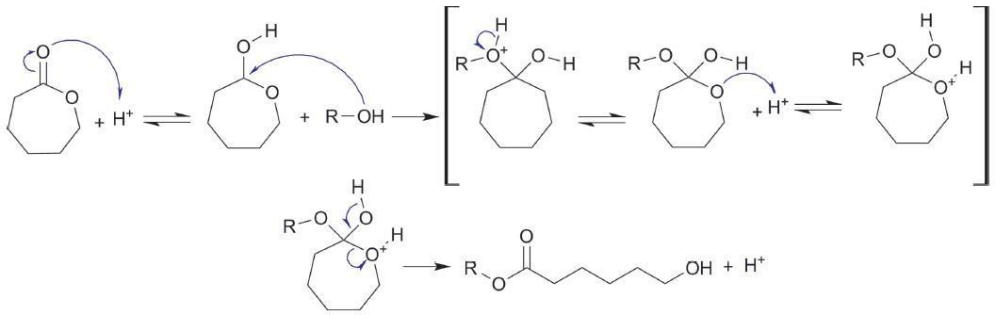

Figure 6 Mechanism of the initiation step for the monomer-activated ROP [37,39]

IV. Coordination–insertion: the most common way of ROP and a pseudo-anionic ROP. The propagation is proposed to proceed through the coordination of the monomer to the catalyst and the insertion of the monomer into a metal–oxygen bond of the catalyst. During propagation, the growing chain is attached to the metal through an alkoxide bond (Figure 7).

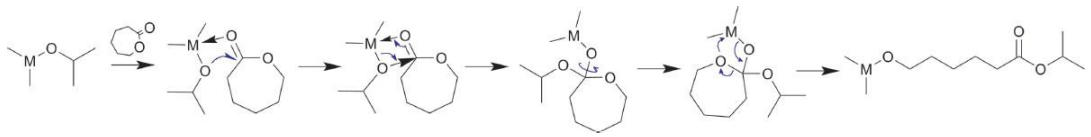

Figure 7 Mechanism of the initiation step for coordination–insertion ROP [39]

Moreover, there are three different catalytic systems used for ROP and reaction conditions:

I. metal-based: consisting of Alkali-based, Alkaline earth-based and poor metal-based catalysts, the latter being mostly used to catalyze the ROP of ε-CL.

II. enzymatic

III. organic systems and inorganic acids.

Concise description of the catalyst systems has been well reported by Labet and Thielemans [34].

Biodegradation of PCL

Before explaining specific biodegradation mechanisms of PCL, it is needed to clarify the definition of this term. Referring to the research by Vert et al. [40] biodegradables, in contrast to bioresorbables, bioerodibles and bioabsorbables, are defined as "solid polymeric materials and devices which break down due to macromolecular degradation with dispersion in vivo -i.e. performed or taking place in a living organism- but no proof for the elimination from the body (this definition excludes environmental, fungi or bacterial degradation)" [40]. Biodegradable polymeric systems or devices can be attacked by biological elements so that the integrity of the system is affected and results in fragments or other degradation by-products, which cannot necessarily move away from the body.

In animals and human bodies PCL is not biodegradable due to lack of suitable enzymes, though it is biodegradable by outdoor organisms (e.g. bacteria and fungi). Biodegradation of PCL starts from the amorphous phase, which is degraded first and results in an increase in the degree of crystallinity while the molecular weight remains constant. Afterwards, cleavage of ester bonds results in mass loss. Temperature plays an important role in PCL degradation, as one can observe end chain scission at higher temperatures while random chain scission occurs at lower temperatures [34] as shown in Figure 8.

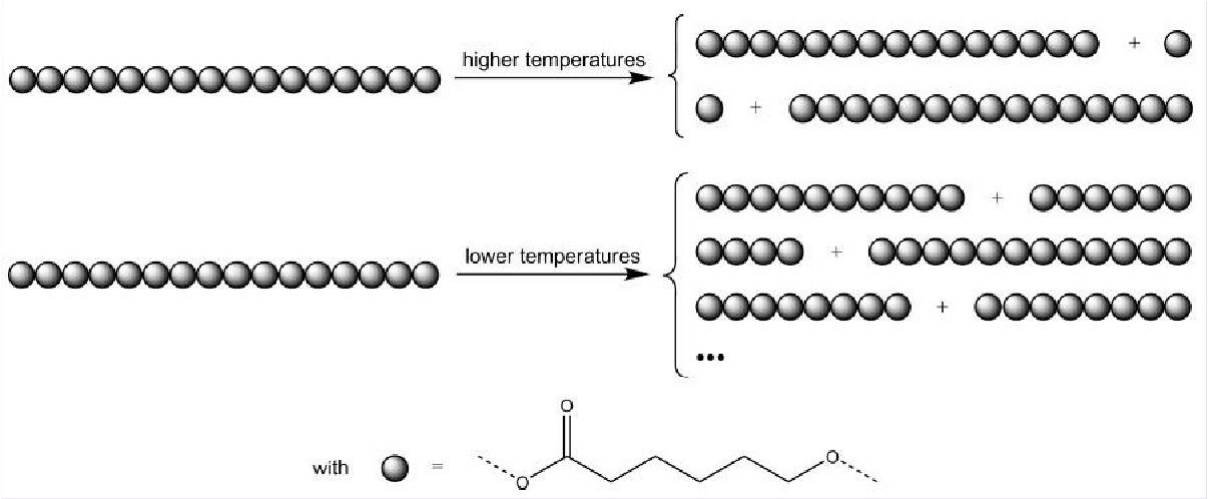

Figure 8 Cleavage of the polymeric chains during the degradation of PCL [34]

Biodegradation process of PCL takes rather long time but it can be catalyzed by enzymes, which results in faster decomposition, or it can be autocatalyzed by the carboxylic acids liberated during hydrolysis [41]. By increasing the rate of hydrolytic chain scission and the production of oligomers and monomers, polymer is thinned over time without changes in the molecular weight. This means that internal bulk of the polymer remains unchanged during

degradation. This property of PCL is advantageous for medical and drug delivery applications, while the probable degradation can be approximately predicted. Depending on the starting molecular weight of the device or implant, PCL has a total degradation of 2–4 years and the rate of hydrolysis can be altered by copolymerization with other lactones or glycolides/lactides [41].

1.4.2. Soft Biomaterials

As already mentioned in section 2.4., soft biomaterials are generally of high water content, inside of which cells are capable of residing. These soft materials can be implemented in regenerative medicine applications such as cell therapy and tissue engineering, allowing mimicry of the range of elastic modulus (E') values associated with the soft tissues of the body [2]. Hydrogels used as biomaterial can be divided to two main categories:

I. Synthetic polymer hydrogels such as polyethylene glycol (PEG)-based materials, such as PEG diacrylate (PEGDA), as well as polyacrylamide (PAAm)-based gels.
II. Naturally-driven hydrogels such as collagen, Hyaluronic acid, alginate, and fibrin

Among the general features of Naturally-driven hydrogels one can point out an innate bioactivity facilitates cell and tissue integration and biocompatibility. Fine -tuned control over molecular weight numbers and distributions, as well as cross-linking densities, allowing for precise modulation of specific mechanical properties such as E' or stiffness are listed among the features of Synthetic hydrogels [2].

Synthetic polymer hydrogels

Synthetic polymers can be mixed with cells and other bioactive factors, e.g. bioactive glass in case of this current master's thesis, in aqueous solution and then be manipulated to form an insoluble, cross-linked meshwork, resulting in a cell-loaded hydrogel [18]. In order to fulfill the expected requirements of hydrogels, in regenerative medicine and medical applications of 3D printing in general, a variety of synthetic materials have already been implemented. Primary advantage of synthetic polymer hydrogels is the ability to have control over their chemical and physical properties, i.e. molecular weight, functional groups, and hydrophobicity/hydrophilicity at a monomer level, leading to manipulate cross-linking rates and mechanical properties more precisely [2]. As already mentioned in part 2.4.2., polyethylene glycol and polyacrylamide are examples of commonly used synthetic polymers, the former

being the most common. As far as PEG is a matter of concern in this research, here a short glance at its properties will be introduced.

Preparation of PEG

PEG, with IUPAC name poly(ethylene oxide) and first produced in 1859, belongs to the group of solid-liquid phase change materials (PCMs) which exhibit many desirable characteristics, such as high fusion heat of 150–180 J/g, low vapor pressure in the melt, chemically inert and stable, and friendly environment [42] Its only drawback is an unacceptably liquid leakage, which can be adjusted by shape stabilized PCMs (SSPCMs) for its thermal storage applications.

There are a series of physical and chemical methods to prepare SSPCMs, such as PEG. Injecting PCMs into higher melting point-polymeric matrix and chemical grafting, blocking and cross-linking copolymerization reaction between the solid frameworks and PCMs are among these methods [43]. Deng and Yang [42] have introduced a simple sol-gel method to prepare hydrogel PEG as well.

Generally speaking, PEG is produced by the interaction of ethylene oxide with water, ethylene glycol, or ethylene glycol oligomers catalyzed by acidic or basic catalysts as shown in Figure 9.

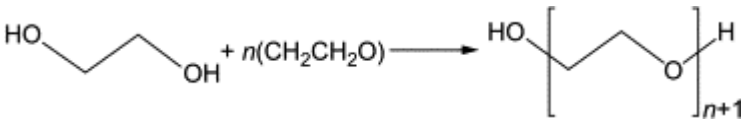

Figure 9 Interaction of ethylene oxide with ethylene glycol oligomers catalyzed by acidic or basic catalysts [29]

PEG has long been used as medical device coatings to control host immune responses or appended to drug constructs to reduce degradation in vivo. It can also be manipulated to form a variety of hydrogels for cell culture and stem cell differentiation. PEG is often chemically modified with acrylate groups to create a photopolymerizable poly(ethylene glycol) diacrylate (PEGDA) in which cells can quickly be encapsulated.

Inherent drawback of PEG is the necessity to artificially preprogram all biological activity, thanks to the lack of natural attachment sites that can interact with cells inside synthetic polymer chains. Thus, in order to support cell adherence, PEG requires chemical immobilization of cell adhesion motifs. This fact puts synthetic polymer hydrogels in lower position compared to Naturally-driven one, which are derived from natural polymers or peptides and can retain their original biological activity in most cases.

In the next part, these naturally-driven hydrogels and their common examples will be introduced.

Naturally-driven hydrogels

I. Collagen

As the most frequently used to function as cell substrate due to being naturally the main component in most tissues [44] and establishment of isolation and purification processes, collagen is an industry-wide naturally driven hydrogel. Collagens, specifically type I, are mainly used as surface coatings and gels for cell culture.

As advantage of using collagen, one can refer to arginine–glycine–aspartic acid (RGD) amino acid sequences, which are inherent to collagen and allow cells to adhere and proliferate via integrin–RGD binding. However, strong cell attachment ability causes limitations upon cell migration and locomotion. Therefore, using almost ∼100% collagen matrices are not recommended [2]. Another important factor is lack of elastin, fibrinogen, laminin, and glycosaminoglycans (GAGs) may lead to biological signaling that can induce unanticipated cellular changes. Plus, presence of hydrophobic peptide motifs in collagen fibers and their ability to exclude water cause decreased function, decreased diffusion of nutrients and gases, and cell death as they are used as implements and cell delivery agents. Though still in use, future collagens must be of hybrid nature in combination with other extra cellular matrix (ECM) components with superior properties.

I. Hyaluronic Acid (HA)

As explained by Allison and Grande-Allen (2006) hyaluronic acid (HA), or hyaluronan, is a versatile non-sulfated GAG consisting of repeating disaccharide units and is present in tissues as a major constituent of the ECM that has shown great potential in regenerative medicine. Chemically modified hyaluronic acid as a useful and robust material that can be cross-linked or loaded with other functional molecules has also been reported [45].

Photo-cross-linking of HA hydrogels is often done by appending methacrylate groups to HA chains, which can undergo free radical polymerization when exposed to ultraviolet (UV) irradiation to form soft hydrogels, referred to here as maleimide modified (MA-HA) hydrogels [2]. Photo-cross-linkable MA-HA hydrogels have been used in many settings as vessel structure bioprinting [28].

III. Gelatin

As a biodegradable natural protein and a promising material in biomedicine, gelatin is a mixture of peptide sequences derived from collagen that has undergone partial hydrolysis. It consists of a high number of different amino acids. The most frequent ones, regardless of their origin, are: proline, hydroxyproline and glycine [46]. It has been applied as a wound dressing material, in gene therapy, food industry, drug delivery and in 3D tissue regeneration. Gelatin can be degraded by enzymes without any non-biocompatible by-products and be dissolved in aqueous solutions easier than collagen, while still maintaining the ability to form simple gels when solutions are brought to low temperatures through hydrophobic cross-linking [47]. It consists mainly out of proteins and is synthesized through basic or acidic hydrolysis of collagen. In general, gelatin resembles conditions of collagen, which is the main component of the natural ECM.

Gelatin is a sensitive protein, it turns into an aqueous solution at a temperature of 37 °C (sol state). This is explainable by the physical interdependency of its molecules, which are interrupted at higher temperatures [48]. As the aqueous solution cools down, the gel builds up.

Nevertheless, its main limitations are low gelation/melt temperature which lies between 30°C and 35°C, which prevents it from being applied in cases below physiological temperatures [49].

As common to all hydrogels, gelatin requires chemical modification, alternative cross-linking techniques, or combination with other proteins or polymers for more appropriate implementation in living systems, such as skin [50].

IV. Alginate

Alginate is a natural anionic polysaccharide that is derived from algae or seaweed. Thanks to its ability to form a hydrogel through an almost instantaneous sodium–calcium ion exchange reaction, it is the best choice for microencapsulation of cells, where easily available and inexpensive alginic sodium salt, or sodium alginate, which is unmodified, is quickly cross-linked into calcium alginate hydrogel microspheres [51].

Like PEG, chemically unmodified alginate is highly inert and its use for cell and tissue culture is limited without incorporating cell-adherent motifs. It must be also noted, that using common reagents to create cell-loaded hydrogel microspheres, such as CaCl2, the crosslinking reagent, as well as sodium citrate and ethylene diamine tetra acetic acid (EDTA), commonly used chelators, has a detrimental effect on cell viability.

Finally, it must be noted that ease of alginate gel formation makes it a widely popular material in medical applications of 3D printing, namely bioprinting, where cell encapsulation is required.

V. Fibrin

Fibrin is used for culture of various tissues types. It consists of fibrinogen monomers that are joined by thrombin-mediated cleavage cross-linking. Its application in medical treatments, such as wound healing or blood clotting is distinguished. However, fibrin gels are used in bioprinting only in less concentrated form to construct scaffolds. They have been reported to demonstrate quick cross-linking rates and robust mechanical properties [40]. Fibrin-collagen blend to bioprint hydrogels containing stem cells over full thickness wounds to accelerate skin regeneration [52].

1.5. Biomaterial Features

In this section, general notions that are connected to the use of biomaterials in medical application of 3D printing will be introduced and briefly discussed.

Materials that can be mixed with cells to construct the backbone of a hydrogel must be manipulated from the monomeric/un-cross-linked form to the polymeric/cross-linked by inducing physical or chemical bonding through environmental changes (such as pH, temperature, and ionic concentration), enzymatic initiation, or photopolymerization [2]. Hydrogel are highly adaptable biomaterials for 3D printing technology and generally characterized by excellent porosity for diffusion of oxygen, nutrients, and metabolites and can be further processed under cell-friendly conditions with almost no irritation, inflammation, or products of degradation [53].

Suitable hydrogel must fulfill four interdependent principles. It must:

I. Be biocompatible, nontoxic to cells, and produce little to no immune response upon implantation
II. Have favorable biodegradation kinetics that matches and supports the cells' intrinsic ability to produce a tissue-specific ECM
III. Exhibit some degree of biomimicry to the intended tissue type, such that the implanted construct can serve some interim functionality as the cells within develop into fully functional tissue

IV. Have sufficient structural and mechanical properties in order to retain its 3D structure and volume over a period of time relevant to tissue regeneration

Apart from these biological considerations, one must consider other processing requirements for the use of hydrogels in bioprinting, which belong to the notion of printability. These include:

I. Rheological properties, such as viscosity and shear-thinning,
II. The mechanism by which the hydrogel is cross-linked to form a stable matrix

In the following parts above-mentioned principles will be discussed in more details.

Though the concentration of this research is on printability of polymers and hydrogels in 3D bioprinting, there is a need to introduce briefly general biological properties that are related to 3D bioprinting and important criteria that play a vital role in making a hydrogel suitable for tissue development.

1.5.1. Biocompatibility

Biocompatibility relates to the overall safety of material for use in an organism and is defined as the ability of a material to perform with an appropriate host response in a specific application, for instance in an in vivo experimental examination of the peri-implant and host responses determining the ultimate performance of a material within a biological environment [40]. In case of permanently implanted devices/implants, minimizing interactions between material and tissue is a primary goal. Furthermore, stability of the interaction of the living environment and the material is a point of concern as well, especially in long-term therapies. In general, one can say, that biocompatibility means proving desired function with respect to a medical therapy, without eliciting any undesirable local or systemic effects in the recipient or beneficiary of that therapy, but generating the most appropriate beneficial cellular or tissue response in that specific situation, and optimizing the clinically relevant performance of that therapy [40].

1.5.2. Biodegradation Kinetics

Hydrogels, like the body's own ECM, are considered as dynamic materials that can be remodeled and degraded over time [2]. Degradation of these polymeric scaffolds occurs primarily via enzymes (most natural polymers and functionally modified synthetic polymers), hydrolytic reactions (synthetic polymers), or ion exchange (e.g., alginate), each with a various kinetic profile. On the other hand, enzymatic reactions are more specific and controllable, as the rate of enzymatic degradation depends on the number of cleavage sites on the polymer and concentration of enzymes in the surrounding environment [44].

1.5.3. Biomimicry

It refers to the ability of hydrogel to mimic human body tissues which are generally divided to four basic types:

I. Epithelial;

II. Muscular;

III. Nervous;

IV. Connective.

Related examples can well define, how each of the above-mentioned tissue types can be biologically mimicked. Further investigation of this issue is beyond the interest if this research. Though as a relatively simple example, one can refer to hydrogels modification to take on a more biomimetic composition, considering the transition from soft to hard tissue at the tendon/ ligament–bone interface [2].

1.5.4. Structural and Mechanical Properties

In case of hydrogel, the structural and mechanical properties must be considered in the context of stability as a substrate for printing and also in the context of the target tissue. Selecting a hydrogel, which is viscoelastic by nature, must be aligned with relevant and desired mechanical properties essential to the function of tissue, ranging from soft tissues such as fat, skin, and muscle, to harder tissues such as cartilage and bone. Plus, structural integrity plays another important role as bioprinting involves a layer-by-layer deposition process for the construction of a volumetric tissue construct. This property has much to do with the polymer chosen, molecular weight and concentration of polymer used, and degree of gelation/crosslinking attained. Finally, one must take into account that all these structural and mechanical properties are not fixed, as the degradation of the hydrogel structure leads to a progressively weaker scaffold. Moreover, there can be a significant amount of swelling or contraction depending on hydrogel composition, cell type, and cell density. According to one study, collagen gels can contract up to 50% and PEGDA gels can swell up to 200% *in vitro* [55]. The amount of deformation is an important parameter when considering the final structure of a bioprinted construct.

2.6. Printability

Before explaining main printability principles of hydrogels, it must be considered that in each of the printing technologies explained in part 2.3., hydrogel is treated with slight differences.

In inkjet-based and extrusion-based systems the use of a nozzle for deposition of the hydrogel material, makes rheological properties, such as viscosity and shear forces, an important consideration. However, laser-based printers use nozzle-free devices, therefore require other properties than rheology.

1.6.1. Rheological Properties

Rheology is the study of material flow in response to an applied force. While this is a complex field involving a deep understanding of fluid mechanics and non-Newtonian physics, two basic concepts that should be considered when attempting to use a hydrogel for bioprinting are:

I. The material's viscosity
II. Shear-thinning properties.

These two properties are especially important to the nozzle-based inkjet and extrusion printing methods.

By definition, viscosity is the degree of material's resistance to flow upon force, i.e. pressure in printing technologies. To be more specific, Malda et al. [4] explain the role of viscosity in case of inkjet printing. In this method, small amounts of air pressure are formed within the printing syringe via vaporization (thermal inkjet printing) or acoustic pulsation (piezoelectric inkjet printing) of the cell-laden suspension within. Air pressure is created by these high-frequency thermal or acoustic pulses to propel liquid through the printing nozzle in a drop-on-demand fashion. Inkjet printers deposit very small volumes (<100 pL) and require hydrogels in their precursor (uncross-linked), low-viscosity state (ideally below 0.1 Pa·s).

Extrusion-based systems deposit continuous hydrogel filaments (as opposed to inkjet droplets) by applying pressure in a pneumatic, piston-driven or screw manner. Higher viscosity of hydrogels (30 to 6×10^6 mPa·s) in these systems is a must, as they are devised by the nozzles on the order of tens to hundreds of microns and leakage of hydrogels through nozzles must be avoided [56].

Hydrogels are non-Newtonian fluids but when it comes to optimization of nozzle-based dispensing, one must consider the Poiseuille equation (1) as a guideline:

$$\Delta P = 8\mu LQ/\pi r^4 \qquad (1)$$

where ΔP is the difference between the pressure applied to the fluid and the ambient pressure, μ is the material's viscosity, L is the length of the nozzle tip, Q is the flow rate (or "scan speed"), and r is the radius of the nozzle tip.

The category of LIFT printing systems, though, can employ hydrogels with a wide range of viscosities (1–300 mPa·s), as they do not function based on ejection through a nozzle [57].

Shear thinning, defined as the inverse relationship between shear rate and viscosity, is a non-Newtonian behavior of some fluids such as polymers, which are shear-thinning materials because when they experience shear stress, their entanglements stretch and become more uniformly aligned parallel to the applied stress, thus decreasing the viscosity [4]. Shear thinning is a property of high-viscosity polymer networks through an orifice, which is of particular importance in extrusion-based printing systems. Hydrogels have similar (high) viscosities within a printing syringe and after deposition, which provide good mechanical strength while also possessing a transitional (low) viscosity state that allows for the extrusion of the material through the nozzle.

It is worth mentioning that there are other rheological properties, contributing to the printability of a hydrogel. Yield stress, surface tension, and thermal conductivity are among these extra rheological properties. Importance of rheological properties in medical applications of 3D printing originates from the fact that by paying enough attention to them, researchers will be able to design hydrogels with higher printing fidelity, decrease total fabrication time, and make more informed modifications to hydrogel composition.

1.6.2. Gelation and Cross-linking

This part explains gelation and Cross-linking, which are the most important feature contributing to a hydrogel's overall function. Adjacent and overlapping polymer strands help hydrogel form its semisolid state by complex interactions. Entangled polymeric meshwork can be reached by cross-linking and can ultimately be used to encapsulate cells and other biological compounds. In this respect, three requirements must be fulfilled by a hydrogel to be applied to bioprinting:

I. it must have a relatively quick gelation time such that subsequent layers can be immediately deposited on top;
II. the mechanism of crosslinking should be noncytotoxic

III. the cross-links formed should be stable in an aqueous environment at physiologic temperature and pH

Cross-linking methods can be broadly divided into:

I. Physical cross-linking (which includes ionic interactions and hydrogen bonding)
II. chemical cross-linking (which forms covalent bonds secondary to photoinitiation or enzyme catalysis)

Based on this division, we can categorize major classes of hydrogels in terms of cross-linking methods:

I. Thermosensitive hydrogels (Collagen I, Agarose, and Pluronic®, Gelatin)

Hydrogels of this category are formed secondary to conformational changes in their constituent monomers at a certain temperature, which is called the critical solution temperature and might be upper or lower in different hydrogels. It helps identify where exactly, i.e. up or down to this critical temperature, the insoluble semisolid gel forms. Gelatin, for example, has an upper critical temperature around 30°C, meaning that gelatin solutions are soluble liquids above 30°C and insoluble gels below 30°C. The process which is known as solution-to-gel transition, is usually rather gradual depending on distance from the critical solution temperature

II. Ionically cross-linking hydrogels (Alginate)

Hydrogels of this category are formed by physical interactions between ions and polymer side chains. Alginate forms cross-links via hydrogen bonding. When divalent cations (e.g., calcium, barium and strontium) are introduced into the environment, they compete with monovalent cations (e.g., sodium) to allow for the crosslinking of carboxylic acid groups on adjacent glucuronic acid blocks. Cross-linking using this method is instantaneous.

III. Enzymatically cross-linking hydrogels (Fibrin)

Hydrogels of this category are formed by enzyme-mediated covalent bonding, often between lysine and glutamine residues on adjacent polymer strands.

IV. Photopolymerizable hydrogels (hyaluronic acid, gelatin, and PEG)

Hydrogels of this category are formed when free radicals propagate through reactive functional groups (often C═C bonds) to form stable cross-links. In order to catalyze this reaction, photo initiators are often employed to generate free radicals when exposed to UV-wavelength light. Reactive functional groups, such as thiols and acrylates, can be substituted onto polymers for participation in covalent bonding. This method, which induces polymerization on the order of

seconds to minutes, has been employed for polymers that would not readily form cross-links via other means.

2. MATERIALS AND METHODS

The aim of this research is to make a comparison between pure polycaprolactone (PCL) and a combination of polycaprolactone and polyethylene glycol (PCL-PEG) blend together with alginate dialdehyde gelatin hydrogel (ADA-GEL) to fabricate 3D scaffolds with sequential bioprinting process. Experiments consist of three major parts, namely Hard Phase Evaluation, Hard Phase Scaffold Characterization and Hard-Soft Phase scaffolds to characterize scaffolds and tackle printing challenges.

I. Hard Phase Evaluation:

- Using FTIR spectrometer; to evaluate the material composition of structures.
- Contact Angle Measurement; sessile drop method using ultrapure water to determine resulting contact angle.

II. Hard Phase Scaffold Characterization:

- Strut and Pore size; using bright field microscopy and ImagJ software to analyze images.
- Porosity; measuring the density of the samples using density kit of analytical balance.
- Mechanical Testing; compression testing machine to determine compressive stiffness of the scaffolds from the initial linear region of the stress–strain curve.
- Degradation study; incubating samples in balanced salt solution to examine mass loss later.
- Scanning Electron Microscopy (SEM) to visually characterize the morphology of PCL and PCL-PEG scaffolds.

III. Hard-Soft Phase scaffolds

- Printing a 4-layer scaffold of the possibly best PCL-PEG blend, as determined to be the best ratio of bend through material characterization, and covalently cross-linked ADA-GEL.

2.1. Materials for scaffolding

PCL and PCL-PEG blend

In order to print scaffolds of pure PCL, 10 grams of PCL granules (Mn = 40,000-50,000), purchased from Sigma Aldrich, St. Louis, MO, USA [64], with the melting temperature 56-64 °C according to the product specification and 60°C according to the literature, were filled in

the cartridge of the BioScaffolder 3.1™ (GeSiM mbH, Großerkmannsdorf, Germany) [65] and heated up to 110 °C for about 30 minutes before starting the printing process in order to assure homogeneous temperature distribution within the melt. Melt index according to the product specification is 1.8g/10min.

In order to prepare bioink to print scaffolds of PCL-PEG blend, PCL granules (Mn = 40,000-50,000) and PEG (Mn = 7000 to 9000), purchased from Sigma Aldrich, St. Louis, MO, USA, with the melting temperature 61-64 °C according to the product specification, were mixed in two different ratios, i.e. 80-20 and 70-30 directly in the cartridge of the BioScaffolder 3.1™ and depending on the amount of PEG, heated to 80-110 °C and manually mixed with a spatula to be homogeneously distributed. Blends were heated for about 30 minutes before starting the printing process in order to assure homogeneous temperature distribution within the melt (Figure 10).

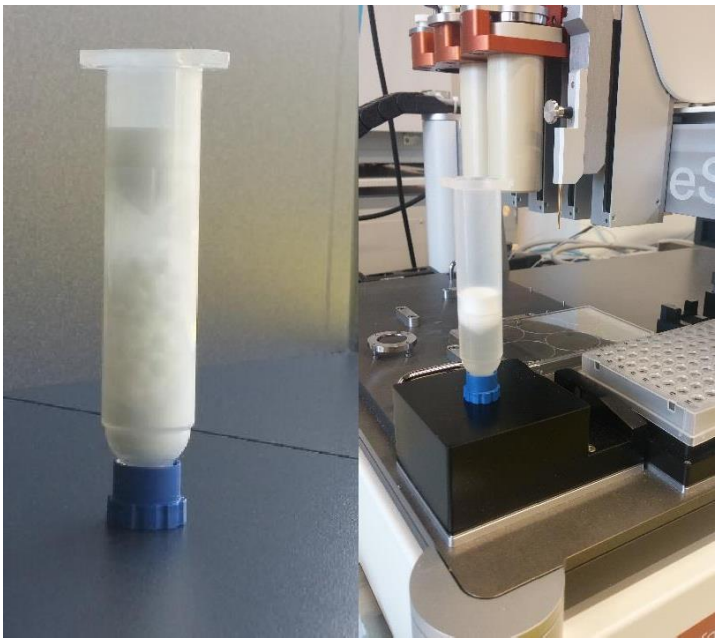

Figure 10 (from left to right) i) PCL-PEG blend with ratio of 80-20, ii) covalently cross-linked ADA-GEL prepared to be printed

ADA-GEL

As described in the sub-section 2.4.2., gelatin suffers from poor kinetic and temporal limitations, although its properties, as in the case of collagen, makes it the most similar soft material to ECMs. In order to overcome these limitation, gelatin can be crosslinked to alginate dialdehyde, which is the partially oxidized product of alginate through the oxidizing agent sodium-periodate [49]. With this treatment the degradation behavior of alginate can be

improved. The resulting ADA has the advantage of faster degradation compared to alginate due to its reduced molecular weight as a result of the partial oxidation process and the thus higher porosity [58]. Here the role of sodium-periodate is to cleave adjacent glycols of the alginate and forms the aldehyde derivatives. During the reaction every α-glycol group uses one periodate molecule. The rate of this reaction is thereby dependent on the stereochemistry of the glycol group. In ADA two aldehyde groups are built at every oxidized monomeric unit through the division of the carbon-carbon bonds. At the repetitive units, the hydroxyl groups of carbon 2 and 3 are oxidized by sodium metaperiodate [49]. The yield of oxidation in an ethanol-water mixture lies at 50- 60 % as reported in literature [59]. ADA which has been used in scaffold fabrications was fabricated during a 14-day preparation process with several steps, following the protocol of Ivanovska et al. [60].

Having in mind that cells will be further applied in ADA, it must have been covalently crosslinked with gelatin to improve the cell adhesion and the cell-material interaction. Such an application of covalently cross-linked ADA-GEL as an ink for bioprinting in different biofabrication approaches due to its mild gelling conditions and tunable properties has been well reported in the literature [61].

The hydrogel used for Hard-Soft Phase scaffold fabrication was a stock solution of 7.5 % (w/v) highly viscous and fibrous ADA solved in 5 ml of Dulbecco's Phosphate Buffered Saline (DPBS) purchased from Sigma Aldrich, St. Louis, MO, USA, with a magnetic bar over Standard Magnetic Stirrers 120V (VWR®, Brooklyn, USA) with the stirring level set at 4, at room temperature and with an aluminum foil cover to avoid vaporization. The process took roughly 2 hours. GEL preparation consisted of solving gelatin from porcine skin purchased from Sigma Aldrich, St. Louis, MO, USA, in 5 ml of pure water, with the concentration of 7.5% (w/v), followed by heating up the mixture up to 50 °C for 15 minutes and afterwards cooling it down to 37 °C.

The 7.5% (w/v) aqueous solution of gelatin was dropped slowly into ADA solution (7.5 % (w/v)). These two were crosslinked for 8 minutes with a magnetic bar on magnetic stirrers. The resulting covalently cross-linked ADA-GEL was filled in a plastic cartridge with the capacity of 30 ml (Nordson Deutschland GmbH, Erkrath, Germany), as a gel reservoir for printing. This cartridge was mounted to the left cartridge of the Bioscaffolder 3.1™, which is suitable for materials without the need of being heated up. Among the three available cartridges, left cartridge was chosen because of it appropriate distance from the right cartridge, containing

thermoplastics and normally heated up to min. 80 °C, therefore leaving the middle cartridge free to function as a shield to prevent heat transfer.

2.2. Printing process

2.2.1. 3D BioScaffolder 3.1™ machine details

The BioScaffolder 3.1™ is a rapid prototyping or tissue printing for 3D cell culture and regenerative medicine. It is pressure-controlled by the accompanying F-Box, which is an external electronic control unit with embedded computer and connects to sensor cables, compressed air and liquid (water) system. Its maximum substrate-holder size is 31 cm x 20 cm. Devised with three independent multi-Z-drives (Axis A, C, E) and separated drive for piezo dispensing, it can print various materials - ranging from naturally-driven hydrogels (e. g. collagen, alginate), Bioglass, bone cement paste, biocompatible silicones to thermoplastic polymers (polycaprolactone, polylactic acid etc.) - at different pressures (100 – 700 kPa; (1 – 7 bar, according to the device specifications, up to 550 kPa in practice) and temperatures (max. 120 °C) without exchanging cartridges. Printing of either simple or complex geometries is possible through the import of CAD data (STL-files). Figure 11 shows a picture of BioScaffolder 3.1™, GeSiM mbH, Großerkmannsdorf, Germany, and its multiZ-drives.

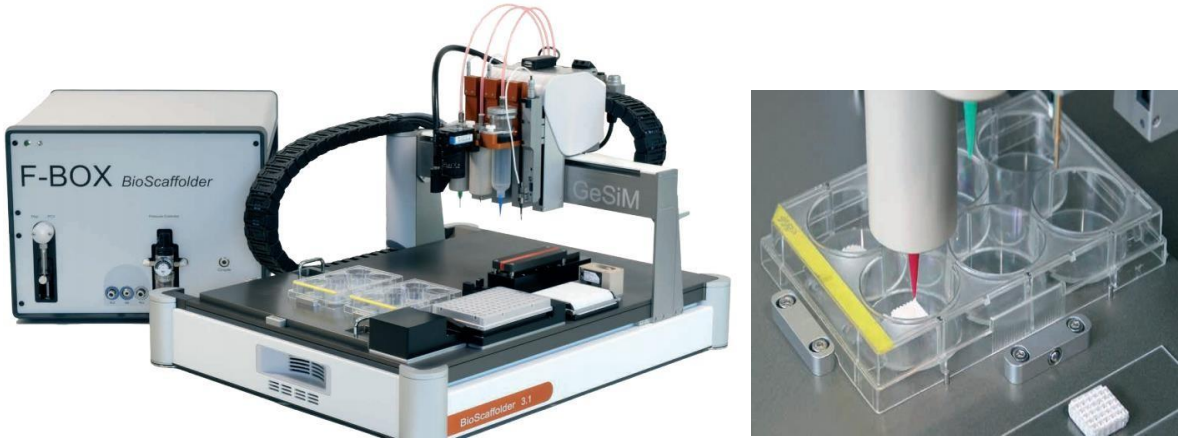

Figure 11 (left to right) BioScaffolder 3.1™ (GeSiM mbH, Großerkmannsdorf, Germany); multiZ-drives (spindles) of the BioScaffolder 3.1™ while printing on the well plate used as printing substrate by heating cartridges [65]

Table 1 reviews features offered by The BioScaffolder 3.1™.

Table 1 BioScaffolder 3.1™ Specification [65]

Features	Applications
piezoelectric inkjet printing (microdispensing)	cell suspensions or to coat scaffolds with matrix proteins
“organ printing” (Printing of live cells)	Embedding them in scaffold material or seeding by piezo spotting
Z-sensor	Measurement of substrate heights plus a XYZ tip calibration tool for automatic alignment of dispensers
Tip cleaner	Wiping off excess paste
Extra Options	Picking samples from a heatable plate Piezoelectric GESIM nanoliter pipettor (heatable and non-heatable) Washing/Drying unit
Device competence	*Plotting of conductive polymers as sensor material or as coating for medical devices *Dispensing of photosensitive material and UV crosslinking (UV lamp + optical fibre) *High-voltage unit for directed melt-electrospinning (MES) to produce fine polymer meshes

2.2.2. Printing Workflow

Firstly, the F-Box and computer were turned on and the pre-set configuration was uploaded to the Scaffold Generator Software (GeSiM mbH, Großerkmannsdorf, Germany), through which the printer was initialized in order to set all z-Drivers to the right starting position.

Secondly, a 6-well culture plate was placed under the z-Drivers to function as an equal-surface substrate for printing scaffolds. In this stage, the tip measurement was done by z-Sensor of the printer, commanded through Run section of the GeSIM software to define the substrate height for the printer. Thirdly, as thermoplastic materials must be heated to be melt, temperature of the cartridge with PCL or PCL-PEG blend was set to the appropriate temperature, which was chosen empirically regarding achieving appropriate rheological properties while printing. Processing temperature was set at 110 °C to 115 °C for pure PCL, 100 °C foe PCL-PEG 80-20 and 85 °C to 90 °C for PCL-PEG 70-30. A conic aluminium nozzle (Vieweg GmbH, Kranzber, Germany), through which heated materials were extruded, with a diameter of 250 µm, according to the product specification, was used. Its diameter was double-checked by a light microscope (Stemi 508 ZEISS, Oberkochen, Germany) to be sure about its exact size, as it might be eroded or modified through multiple usage (Figure 12). The observed diameter was about 33 µm bigger than given product specification.

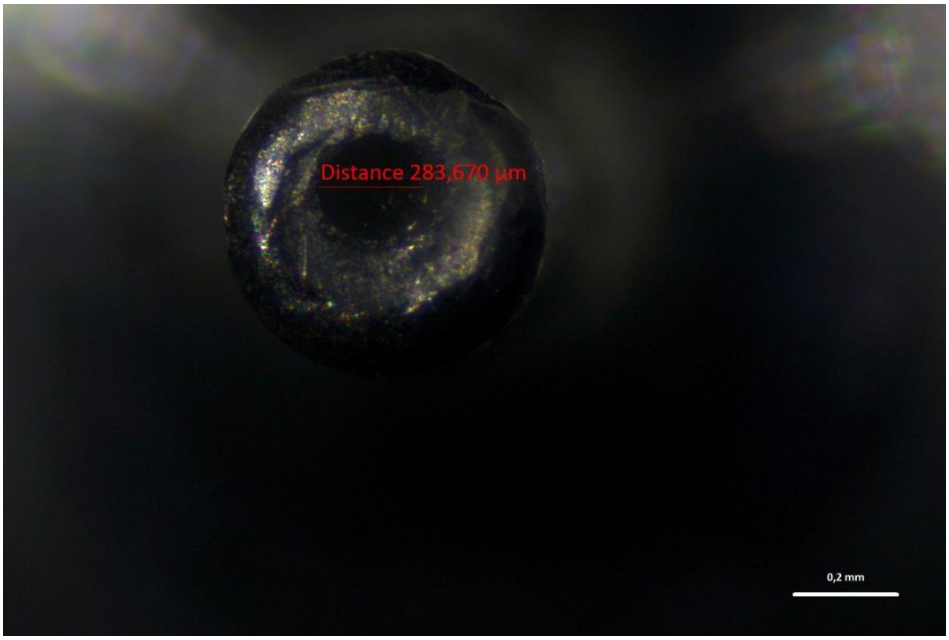

Figure 12 measured conic aluminium nozzle diameter by light microscope ZEISS Stemi 508, ZEISS, Oberkochen, Germany

Heat insulation shield maintaining a homogeneous temperature and low temperature drop to the nozzle footprint was mounted previously to the button of the z-Driver.

In case of ADA-GEL, plastic Precision TE Needle 22 Gauge X 1/2" Blue, (OKInternational, California, USA) , with diameter 200 µm was used.

Afterwards, printing process was started using optical and mechanical calibration tools for the automatic offset compensation between the tools and the ground level. The scaffold-generation

poses the last step, before the scaffold-printing process can be carried out. The embedded 'Scaffold Generator' of the GeSiM software enables the printing of simple forms consisting of single strands/struts up to complex geometries based on CAD data by importing stl-files or directly designing simple geometries through software setting. Post-printing process was required in case of printed ADA-GEL, which consisted of crosslinking them with 0,1 M $CaCl_2$.

As the viscosity of the biomaterial is a major factor in the biofabrication process, pressure and velocity of the cartridges must be adapted to the materials.

2.3. Design of 3D Scaffolds

The scaffold design was generated with the GeSiM 'Scaffold Generator'. The scaffold cubic geometry was set to 10 mm x 10 mm with height layer of 90 µm. Scaffolds were built of 14 double layers, meaning each layer consists of two struts. Subsequent layers were positioned in a 90° pattern with parallel lines entailing equal interspace. Table 2 shows range of printing parameters, which were obtained by a trial-and-error approach, backed up by some similar attempts in the literature [5].

Table 2 Printing parameters to print ADA-GEL, pure PCL, PCL-PEG 80- 20 and PCL-PEG 70 - 30

Scaffolds specification				
Printing parameters	**ADA-GEL**	**PCL**	**PCL-PEG 80 - 20**	**PCL-PEG 70 - 30**
Pressure [kPa]	60 - 80	530 – 550	510 – 530	450 - 480
Temperature [°C]	Room temperature	115 - 100	100	85 - 90
Speed [mm/s]	3 - 5	1	1	2
Nozzle diameter [µm]	200	250	250	250
Shape/Form	Quadrat	Quadrat	Quadrat	Quadrat

Side length [mm]	10	10	10	10
Number of double-layers	14	14	14	14
Layer-height [µm]	90	90	90	90
Strands/Struts p. layer	2	2	2	2
Outline offset [mm]	0.04 – 0.02	1.02 – 1.5	1.02 – 1.5	1.02 – 1.5
Interlayer pause [s]	8 – 10	1	1	1
Start break [s]	0	0	0	0
End break [s]	0	-0.2	-0.2	-0.2

Lowering the temperature for PCL-PEG 70 – 30, though compensated by increasing the speed was based on the processing temperature proposed by Hoque et al. [11]. This is due to the fact that afterward sequential processing of hydrogel or possible cell solution requires lower temperature to keep cell viability. Image of a sample printed scaffold is shown in Figure 13.

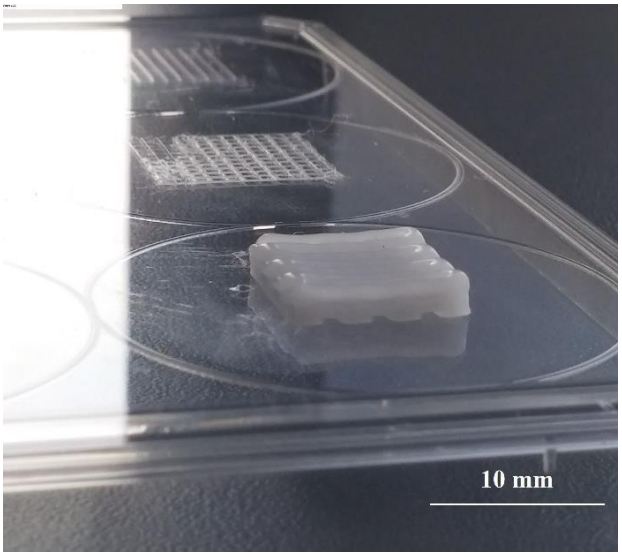

Figure 13 Sample printed scaffold of pure PCL

2.4. Characterization of the Scaffolds, results and discussion

In as far as the printing experiment regards comparing Hard Phase and Hard-Soft Phase scaffolds, which mimic human body tissues, this set of characterizations evaluate chemical properties and structural design of each component.

2.4.1. Characterization of the Material

Fourier Transformed Infrared (FTIR) Spectroscopy data

In order to evaluate material composition, separated planar structures of pure PCL, PCL-PEG 80-20 and PCL-PEG 70-30 were printed by BioScaffolder 3.1™. Number of struts/ layer -only one layer- was set to 30. Using a FTIR spectrometer (IRAffinity-1S Shimadzu, Kyoto, Japan) the characterization was run. Wave number range was set from 400 cm^{-1} up to 4000 cm^{-1}. FTIR spectrum was observed in accompanied IRAffinity-1S System Administration software. Spectral data were exported to an excel file, where exact peaks of PCL and PEG were found and compared further to the literature [62]. Figure 3.5. shows a resulting FTIR spectrum of pure PCL depicted by IRAffinity software.

Figure 14 shows the FTIR spectra of pure PCL and PCL-PEG blends. As can be observed, typical PCL absorption bands representing C-C and C-O stretching in the crystalline phase occur between 1163.0 cm^{-1} and 1230.4 cm^{-1}, and the carbonyl stretching C=O and axial deformation of C–C (=O)–O at around 1720.5 cm^{-1} are noticeable for both pure PCL and blends containing PEG in different ratios. Also in case of pure PCL and observable in two other blends, there is a smoothly shifted peak at around 1119.0 cm^{-1}. Slight peaks at around 1051.0 cm^{-1} are close to those attributed to ether groups. There are also two increased peaks, compared to pure PCL, one at 1009 cm^{-1} and the other at 766 cm^{-1}, which can be attributed to C-O stretching from the PEG molecule. Above-mentioned bands correspond to the similar findings in the literature [12,13,63]. As can be conceived from the Figure 15, all materials represent almost the same absorption spectrum, without any new visible peak or new shifts. It affirms the presence of all materials under study in the blends, while rejecting any intermolecular interactions between PCL and PEG.

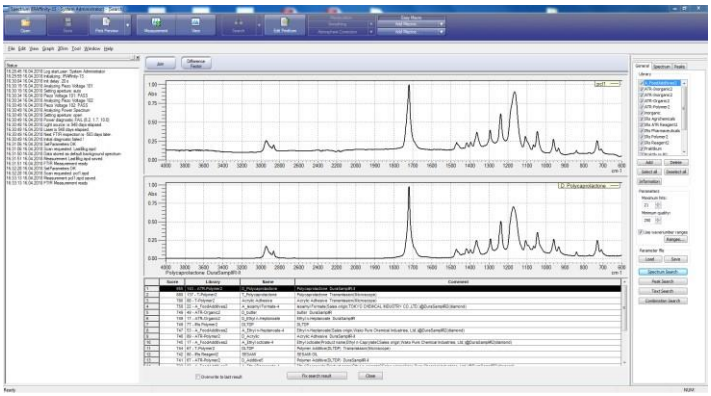

Figure 14 FTIR spectrum of pure PCL depicted by IRAffinity-1S System Administration software

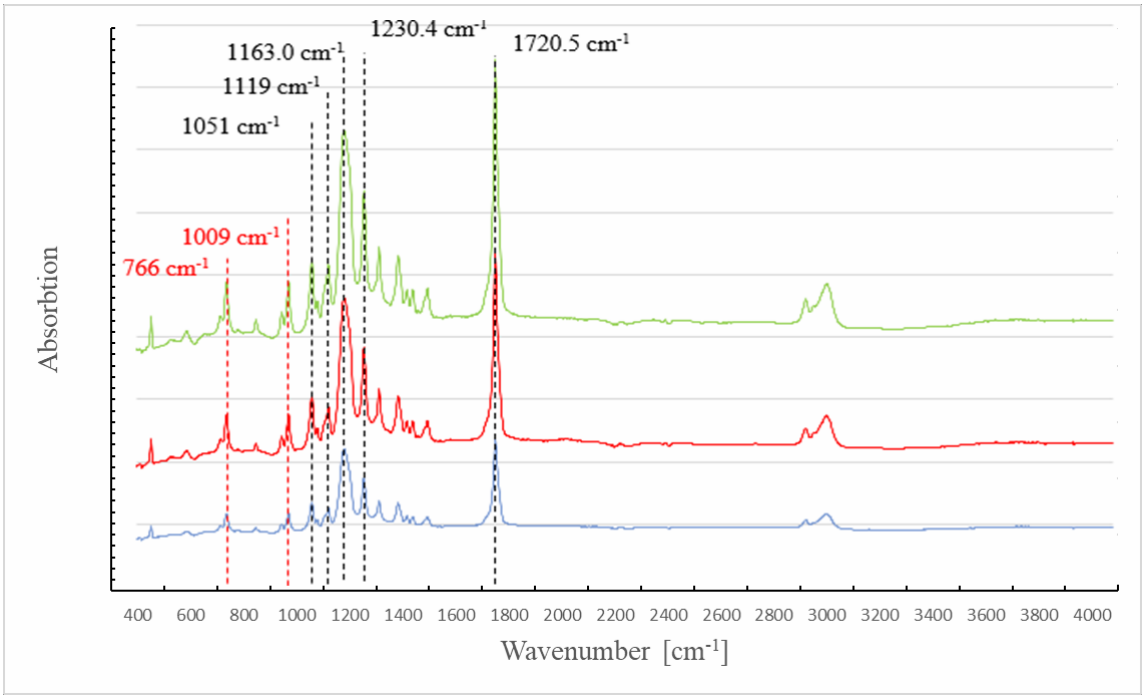

Figure 15 FTIR spectra of pure PCL, PCL-PEG 80 – 20, PCL-PEG 70 – 30 based on data from IRAffinity-1S spectrometer.

Contact Angle Measurement

Sessile drop method using ultra-pure water were used to measure contact angle measurement of planar structures of pure PCL, PCL-PEG 80- 20 and PCL-PEG 70-30, printed by BioScaffolder 3.1™. Number of struts/ layer -only one layer- was set to 30. The resulting contact angle was determined by a drop shape analyzer (DSA30 Kruess GmbH, Hamburg, Germany). Figure 16 represents images of sessile drop after contacting the surface in case of PCL-PEG 80-20, PCL-PEG 70-30 and pure PCL. Table 3 summarizes measured angels after three independent tries for each material combination.

Table 3 Contact Angle Measurement data for pur PCL, PCL-PEG 80 – 20, PCL-PEG 70 – 30

Contact Angle [deg°]			
Num, of measurements	1st	2nd	3rd
Pure PCL	91.8°	91.4°	90.6°
PCL-PEG 80 - 20	81.1°	80.7°	78.7°
PCL-PEG 70 - 30	63.6°	67.3°	69.1°

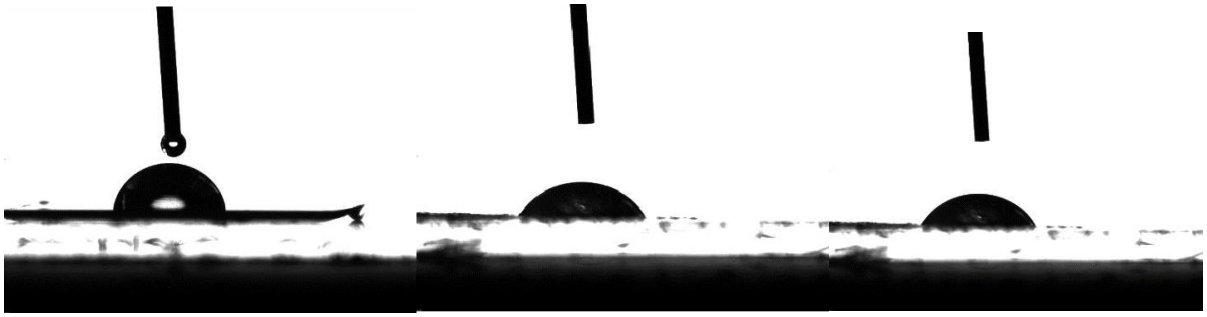

Figure 16 (left to right) Image of sessile drop after contacting the surface in case of i) PCL-PEG 80-20; ii) PCL-PEG 70-30; iii) pure PCL

Hydrophilic properties of PEG results in contact angle reduction, compared to pure PCL. This difference in the contact angle is observable as a very positive effect on the wettability of the samples, as shown in Figure 17.

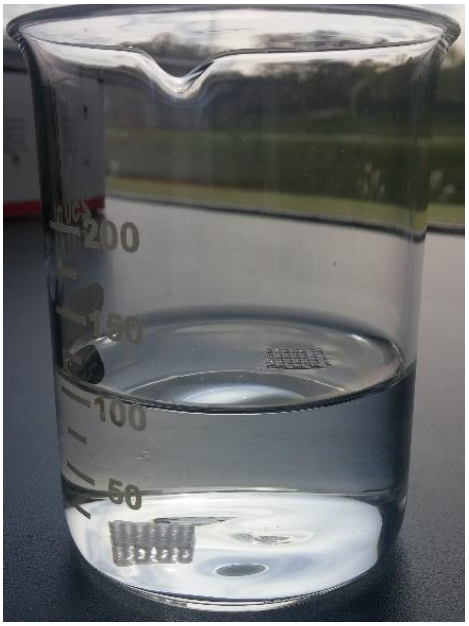

Figure 17 Effect of PEG on the wettability of plotted scaffolds. Pure PCL scaffold is on the surface and PCL-PEG 70 – 30 scaffolds on the bottom of the glass.

The hydrophobic properties of the PCL scaffold inhibit the infiltration of water into the porous scaffold structure. The remaining air causes buoyancy forces, keeping the scaffold on the surface. The scaffold consisting of a more hydrophilic PEG on the other hand, was infiltrated and sank to the bottom. This behavior was also proved by Zehnder et al. [5].

Scanning Electron Microscopy

Following figures illustrate the external and internal morphology of material to observe visually the difference between pure PCL and effect of addition of PEG in case of PCL-PEG 70 – 30 (Figure 18, 19). As can be observed visually from the SEM images, the surface of PCL-PEG blend is smoother than pure PCL scaffold, owing rougher surface in comparison. Thus, the more the ration of PEG in the blend, the smoother the morphology of the scaffold will be. This is due to the hydrogel-type effect that PEG has on a rigid thermoplastic material such as PCL. These images helped determine in greater visual details, that adding PEG to the initial PCL material makes the latter softer and more appropriate in 3D scaffolding, while keeping already-mentoned properties of PCL to print scaffolds distinguishable.

2.4.2. Hard Phase Scaffold Characterization

Strut and Pore Size; Porosity

Using the bright field microscope (Stemi 508 ZEISS, Oberkochen, Germany) and processed in Fiji (ImageJ) as shown in Figure 20, open-source Java image processing program, following images were obtained to determine the width of the struts and pore size from the top scaffold layer in z-direction (Table 4).

The porosity was also determined by surveying the density of the samples using the density kit of the analytical balance (AES-A01, Kern & Sohn GmbH, Balingen, Germany). The weight of the samples was measured in air and after being 10 minutes in ethanol, with ethanol density set to 0.9 g/cm^3 (Figure 21).

Based on the results, the apparent mass density and the geometrical density was calculated. After evaluating the exterior dimensions of the samples using a digital calliper (accuracy of 20 μm), the total open through equation (2):

$$\Phi_{\text{Open Porosity}} = (\phi_{\text{apparent}} - \phi_{\text{geometric}}) / \phi_{\text{apparent}} \ ; \qquad (2)$$

Yielding the results 27.46% of open porosity for pure PCL, 47.61% for PCL-PEG 80 – 20, and 22.51% for PCL-PEG 70 – 30.

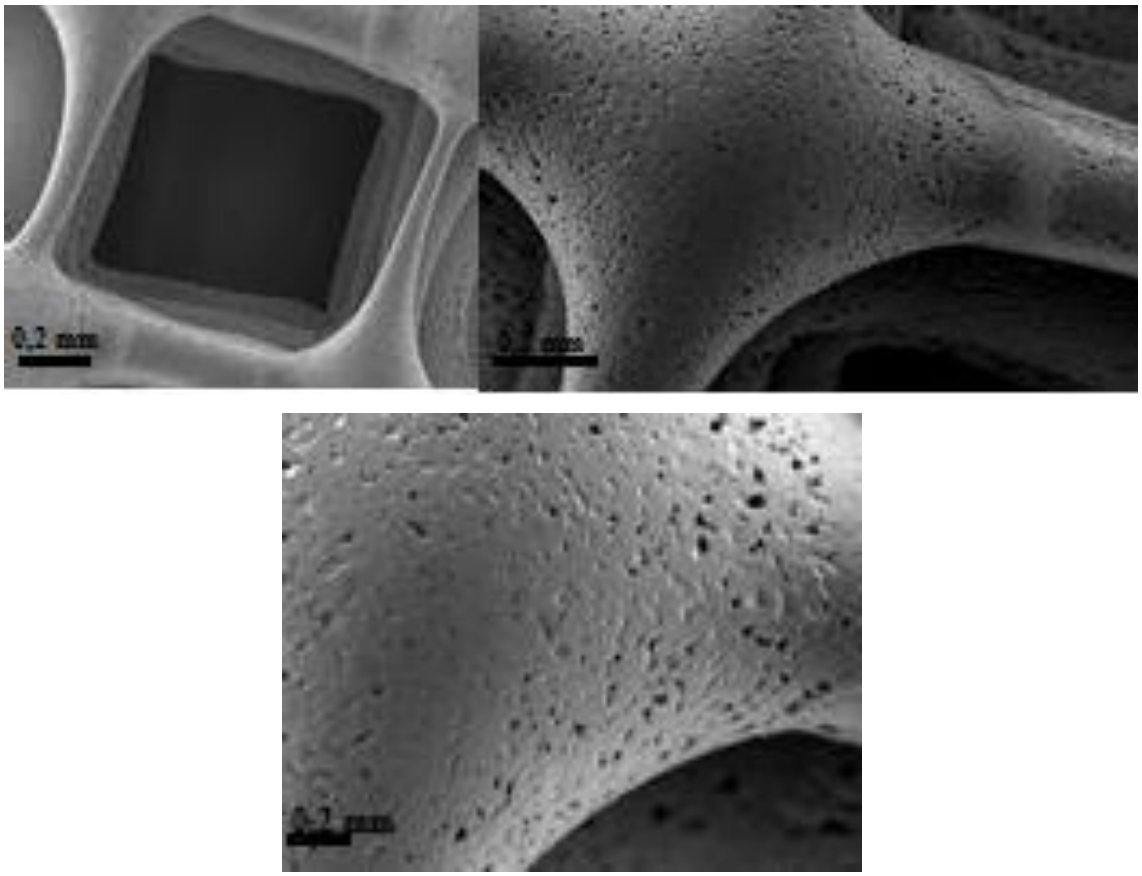

Figure 18 SEM cross-section images of pure PCL

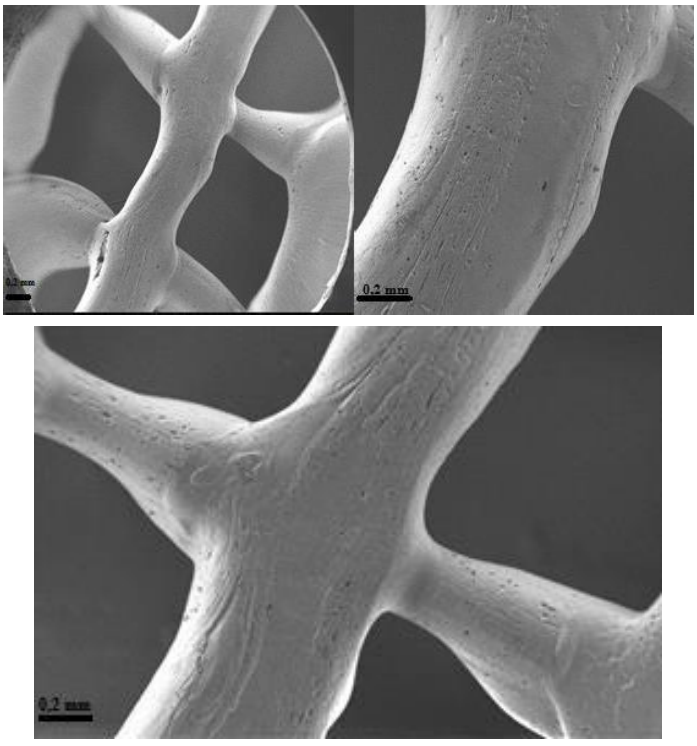

Figure 19 SEM cross-section images PCL-PEG 70 - 30

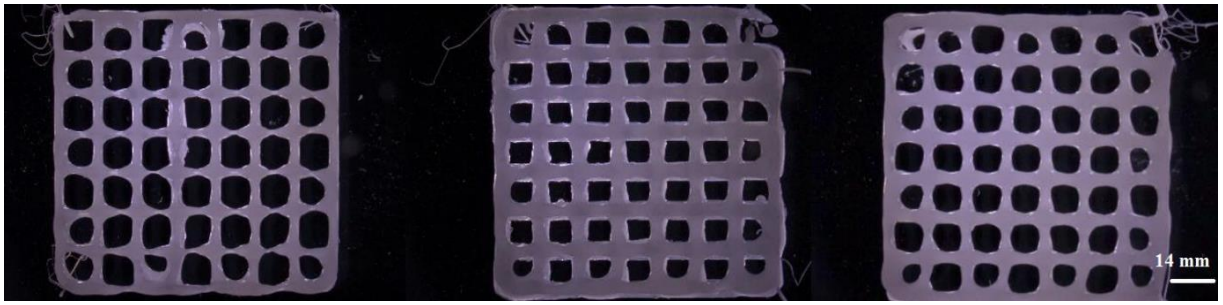

Figure 20 bright field microscopic images of (from right to left) i) PCL-PEG 70 – 30, ii) PCL-PEG 80 – 20, iii) pure PCL by Stemi 508 ZEISS microscope.

Table 4 strut width and pore size of scaffolds i) pure PCL, ii) PCL-PEG 80 – 20, iii) PCL-PEG 70 – 3

	pure PCL	**PCL-PEG 80 – 20**	**PCL-PEG 70 – 30**
Strut Width (µm)	309 ± 69	362 ± 71	298 ± 78
Pore Size (µm)	823 ± 58	750 ± 55	802 ± 63
Porosity (%)	63 ± 4	48 ± 4	65 ± 10

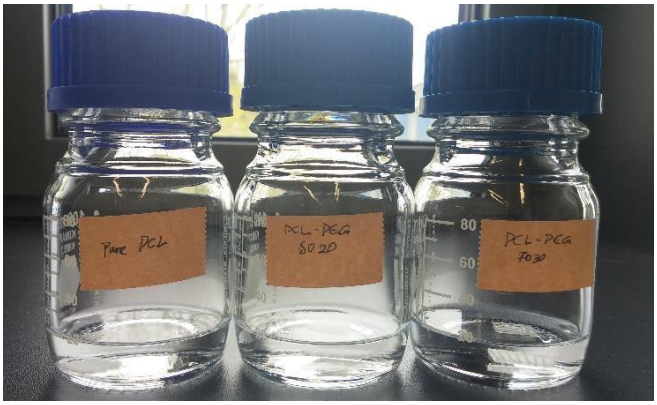

Figure 21 Putting samples into ethanol with density set to 0.9 g/cm^3

As can be inferred from data presented in Table 4, printing parameters and nozzle diameter of 250 µm yield the result of average strut width between 298 µm -362 µm for all three scaffolds. Pore size ranges from 750 µm to 823 µm and the porosity lies between 48% and 65%. Calculated open porosity shows contradicting results compared to Table 4 results, which might be due to ethanol vaporization from gaps in the scaffold during measurement. Another influential factor might be ethanol drop-off from scaffold gaps while weighing them.

Degradation Study

The degradation of the scaffolds was investigated by incubating them in a physiologically buffer solution, Hank's Balanced Salt Solution (HBSS), purchased from Sigma Aldrich, St. Louis, MO, USA, for 72 hours at the temperature of 37 °C at the centrifuge. Scaffolds were weighed before and after the incubation to calculate mass loss, which was the subject of this investigation. As expected through reading of the literature [32], pure PCL proved almost no mass lost after three days of incubation in HBSS. PCL is referred to as a polymer with a total degradation of two years. Presence of PEG in the PCL-PEG blends speeds up the degradation process. PEG has a hydrophilic nature which accelerates its dissolution in the first three days. A similar experiment by Gong et al. [63] supports this result. Blending PCL with PEG enables faster degradation which shows itself after three days of incubation in HBSS, compatible with the ratio of it in the blend, i.e. 15% for PCL-PEG 80 – 20, and 26% for PCL-PEG 70 – 30. Figure 22 shows percentage of mass loss statistically.

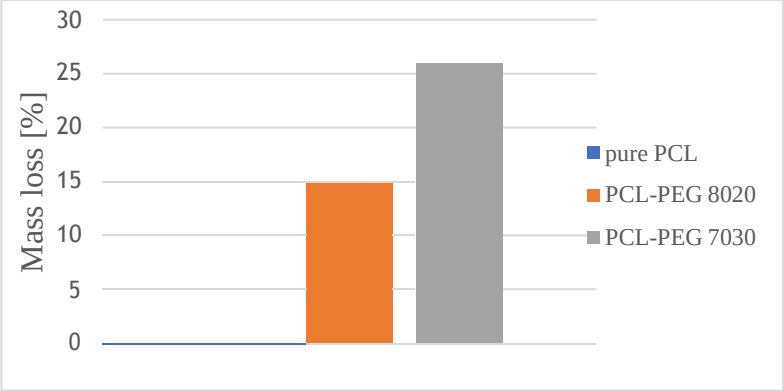

Figure 22 Mass loss [%] of pure PCL, PCL-PEG 80-20 and PCL-PEG 70-30 after 72 hours of incubation in HBSS

2.4.3. Hard-Soft Phase scaffolds

As the purpose of this thesis indicates, the goal is to strengthen the hydrogel, lacking rich mechanical properties as a soft material, with either PCL or PEC-PEG blend. Based on material characterization which was previously done, PCL-PEG 80-20 which proved to have better wettability properties was used for this purpose. The challenge to tackle first, was to optimize printing parameters for ADA-Gel. A set of test scaffolds of only ADA-GEL were printed, whose stability and resolution after printing were supposed empirically to be function of external factors such as changing room temperature during the day, though the laboratory was

under balanced ventilation control constantly. Figure 23 shows initial layer of only ADA-GEL scaffold.

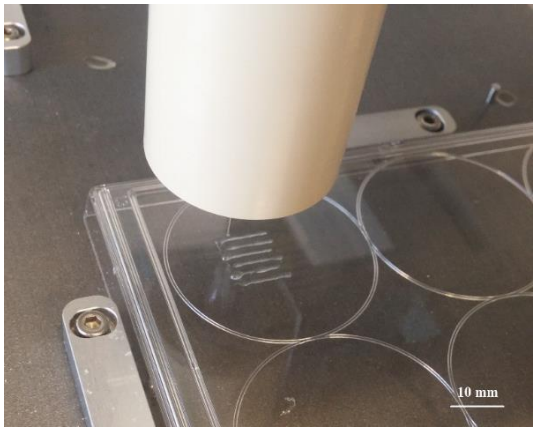

Figure 23 Sample scaffold printing of only ADA-GEL

Sensitivity of ADA-GEL As a prototype for further studies, a two double-layer hybrid scaffold was printed, with first two layers of PCL-PEG 80-20 and second two upper layers of ADA-GEL. Printing parameters were already mentioned earlier in this section. Figure 24 shows the resulting scaffold. Upper two layers of ADA-GEL were ionized by CaCl2 0.1 M for 10 minutes. Afterwards, washed by pure water.

Figure 24 Hybrid scaffold of lower PCL-PEG 80-20 blend and upper ADA-GEL layer

2.6. Limitations

Among many factors which affect the printing process, one can mainly name of temperature, pressure and printing speed. These factors must be adjusted each time for different material compositions. The whole printing process was a trade-off between speed and pressure, while keeping the temperature low as a presupposition for further cell solution. One more important and defining factor is the quality of nozzle, which plays a key role specially in case of printing ADA-GEL. The process of printing ADA-GEL is a challenging task, as the gelation of material inside the cartridge may lead to blocking of the nozzle. As a result, the printing process must

be halted many times to wash the nozzle and reassure a smooth and constant flow of the material. Another unexpected factor was heat transfer between neighboring cartridges. In order to tackle this problem, a mandatory distance between ADA-GEL cartridge and that of thermoplastics was maintained, meaning that practically only right and left cartridge could be used. Quality of the aluminum printing nozzle and its exact diameter played another important role. Low quality of these nozzles can avoid equal heat distribution in the tip of the cartridge, which results in curvy and uneven extrusion of material through it.

Plus, first printed layer of material over the well plate was to some extent thicker than those on upper layers. This can be explainable by the fact that well plate has microscopically uneven and different surface than consequent layers, which are all of the same composition and can make a more even basis for the next to-be-printed layer.

As common to all printing methods, maintaining acceptable resolution is another important factor that must be addressed. Theoretically, strand thickness and interior structure size determine the eventual resolution of the printed scaffold. These two parameters can be subject to other intervening factors such as substrate and homogenously extruded material.

3. CONCLUSION

In this study, 3D scaffolds have been fabricated via additive manufacturing using the BioScaffolder 3.1TM (GeSiM mbH, Großerkmannsdorf, Germany). For the scaffold-printings pure PCL and PCL-PEG blend in two different ratios (8020 and 7030). The scaffold fabrication parameters were optimized in advance to this study and the final structures for each material were analyzed using ImageJ for evaluation of strand and pore size. FTIR and contact angle measurement were conducted for characterization of the material, the porosity was determined and the degradation over 3 days was investigated. Furthermore, a 4 layer scaffold made up of thermoplastics and ADA-GEL was fabricated to strengthen the poor mechanical properties of ADA-GEL.

Moreover, there are some technical considerations which must be taken into account. Behavior of high viscous material such as ADA-GEL can put forward some challenges while printing. The tear-off for example should be set to run faster than in case of thermoplastics.

Additionally, changing the pressure in relation to the start and end position has an impact to the homogeneity of the strand and therefore to the final result of the printing. In case of pure PCL and PCL-PEG blend the pressure was turned just before reaching the start position of the strand,

which lets the material move out of the nozzle in time. The value of pressure is highly dependent on the viscosity of the material and the pre-set pressure. After all, sufficient time for cooling down the deposited material needs to be considered carefully. Even in the case of interlay pause there should be an appropriate time allocated to each layer to take the final shape and cool down. This is done to avoid the so-called sink in effect, which occurs as two strands with low viscosity are printed on top of each other and the upper layer slightly sinks into the lower layer. To reduce the sink in and to avoid merging of the strands, the deposited material needs time for cooling. Thus, an interlayer pause was set for both materials.

Finally, the target-nozzle-distance plays a crucial role in achieving higher printing quality and resolution. Although the calibration of the target via z-sensor and the nozzle via tip-calibrating-tool is automated and accurate, the offset must be adjusted frequently based on empirical evidence.

PCL-PEG prove to be good choice for printing scaffold as they show appropriate wettability and in mixture with PCL, they make it smoother and to an observable extent tunable. They can be controlled at lower temperatures and maintain presupposed cell viability. Plus, they can increase the degradation process of PCL and enable it to act as a rigid, though biodegrabale material for bioscaffolding. These thermoplastics can function as a rigid supporting structure for the main hydrogel, ADA-GEL in this case, which is the carrier of cells.

It remains an interesting task for the future to predict the behavior of high viscous material through computational design of particles. It may reduce the allocated time for trial-and-errors in the laboratory and increases printing efficiency. Moreover, software which is connected to the printing can be enhanced in performance by frequent updates or devising it with new innovating programming or coding approaches.

4. REFERENCES

[1] Shafiee A, Atala A. Printing Technologies for Medical Applications. Trends in Molecular Medicine. 2016;22(3):254-265.

[2] Atala A, Yoo J. Essentials of 3D Biofabrication and Translation. 1st ed. Cambridge: Academic Press; 2015.

[3] Marga F, Jakab K, Khatiwala C, Shepherd B, Dorfman S, Hubbard B et al. Toward engineering functional organ modules by additive manufacturing. Biofabrication. 2012;4(2):1-12.

[4] Malda J, Visser J, Melchels F, Jüngst T, Hennink W, Dhert W et al. 25th Anniversary Article: Engineering Hydrogels for Biofabrication. Advanced Materials. 2013;25(36):5011-5028.

[5] Zehnder T, Freund T, Demir M, Detsch R, Boccaccini A. Fabrication of Cell-Loaded Two-Phase 3D Constructs for Tissue Engineering. Materials. 2016;9(12):887.

[6] Duan B, Hockaday L, Kang K, Butcher J. 3D Bioprinting of heterogeneous aortic valve conduits with alginate/gelatin hydrogels. Journal of Biomedical Materials Research Part A. 2012;101A (5):1255-1264.

[7] Wang T, Kumar S. Electrospinning of polyacrylonitrile nanofibers. Journal of Applied Polymer Science. 2006;102(2):1023-1029.

[8] Visser J, Melchels F, Jeon J, van Bussel E, Kimpton L, Byrne H et al. Reinforcement of hydrogels using three-dimensionally printed microfibres. Nature Communications. 2015;6(1).

[9] Hutmacher D, Schantz T, Zein I, Ng K, Teoh S, Tan K. Mechanical properties and cell cultural response of polycaprolactone scaffolds designed and fabricated via fused deposition modeling. Journal of Biomedical Materials Research. 2001;55(2):203-216.

[10] Declercq H, Desmet T, Berneel E, Dubruel P, Cornelissen M. Synergistic effect of surface modification and scaffold design of bioplotted 3-D poly-ε-caprolactone scaffolds in osteogenic tissue engineering. Acta Biomaterialia. 2013;9(8):7699-7708.

[11] Hoque M, San W, Wei F, Li S, Huang M, Vert M et al. Processing of Polycaprolactone and Polycaprolactone-Based Copolymers into 3D Scaffolds, and Their Cellular Responses. Tissue Engineering Part A. 2009;15(10):3013-3024.

[12] Jiang C, Huang J, Hsieh M. Fabrication of synthesized PCL- PEG- PCL tissue engineering scaffolds using an air pressure- aided deposition system. Rapid Prototyping Journal. 2011;17(4):288-297.

[13] Patrício T, Domingos M, Gloria A, Bártolo P. Characterisation of PCL and PCL/PLA Scaffolds for Tissue Engineering. Procedia CIRP. 2013;5:110-114.
[14] Schuurman W, Khristov V, Pot M, van Weeren P, Dhert W, Malda J. Bioprinting of hybrid tissue constructs with tailorable mechanical properties. Biofabrication. 2011;3(2):021001.
[15] Lee H, Ahn S, Bonassar L, Chun W, Kim G. Cell-Laden Poly(ε-caprolactone)/Alginate Hybrid Scaffolds Fabricated by an Aerosol Cross-Linking Process for Obtaining Homogeneous Cell Distribution: Fabrication, Seeding Efficiency, and Cell Proliferation and Distribution. Tissue Engineering Part C: Methods. 2013;19(10):784-793.
[16] Hull, C.W. Apparatus for production of three-dimensional objects by stereolithography. US 4575330 A, 1986.
[17] Zein N, Hanouneh I, Bishop P, Samaan M, Eghtesad B, Quintini C et al. Three-dimensional print of a liver for preoperative planning in living donor liver transplantation. Liver Transplantation. 2013;19(12):1304-1310.
[18] Kazakis G, Kanellopoulos I, Sotiropoulos S, Lagaros N. Topology optimization aided structural design: Interpretation, computational aspects and 3D printing. Heliyon. 2017;3(10):e00431.
[19] Murphy S, Atala A. 3D bioprinting of tissues and organs. Nature Biotechnology. 2014;32(8):773-785.
[20] Derby B. Bioprinting: inkjet printing proteins and hybrid cell-containing materials and structures. Journal of Materials Chemistry. 2008;18(47):5717.
[21] Catros S, Fricain J, Guillotin B, Pippenger B, Bareille R, Remy M et al. Laser-assisted bioprinting for creating on-demand patterns of human osteoprogenitor cells and nano-hydroxyapatite. Biofabrication. 2011;3(2):025001.
[22] Moon S, Hasan S, Song Y, Xu F, Keles H, Manzur F et al. Layer by Layer Three-dimensional Tissue Epitaxy by Cell-Laden Hydrogel Droplets. Tissue Engineering Part C: Methods. 2010;16(1):157-166.
[23] Nakamura M, Iwanaga S, Henmi C, Arai K, Nishiyama Y. Biomatrices and biomaterials for future developments of bioprinting and biofabrication. Biofabrication. 2010;2(1):014110.
[24] Skardal A, Mack D, Kapetanovic E, Atala A, Jackson JD, Yoo JJ. Bioprinted Amniotic Fluid-Derived Stem Cells Accelerate Wound Healing in Skin. Molecular Therapy. 2012;20:S285.
[25] Bohandy J, Kim B, Adrian F. Metal deposition from a supported metal film using an excimer laser. Journal of Applied Physics. 1986;60(4):1538-1539.

[26] Barron J, Ringeisen B, Kim H, Spargo B, Chrisey D. Application of laser printing to mammalian cells. Thin Solid Films. 2004;453-454:383-387.

[27] Colina M, Serra P, Fernández-Pradas J, Sevilla L, Morenza J. DNA deposition through laser induced forward transfer. Biosensors and Bioelectronics. 2005;20(8):1638-1642.

[28] Guillotin B, Souquet A, Catros S, Duocastella M, Pippenger B, Bellance S et al. Laser assisted bioprinting of engineered tissue with high cell density and microscale organization. Biomaterials. 2010;31(28):7250-7256.

[29] Skardal A, Zhang J, McCoard L, Xu X, Oottamasathien S, Prestwich G. Photocrosslinkable Hyaluronan-Gelatin Hydrogels for Two-Step Bioprinting. Tissue Engineering Part A. 2010;16(8):2675-2685.

[30] Gross R. Biodegradable Polymers for the Environment. Science. 2002;297(5582):803-807.

[31] Kumbar S, Laurencin C, Deng M. Natural and synthetic biomedical polymers. Amsterdam [u.a.]: Elsevier; 2014.

[32] Woodruff M, Hutmacher D. The return of a forgotten polymer—Polycaprolactone in the 21st century. Progress in Polymer Science. 2010;35(10):1217-1256.

[33] Hutmacher D. Scaffolds in tissue engineering bone and cartilage. Biomaterials. 2000;21(24):2529-2543.

[34] Labet M, Thielemans W. Synthesis of polycaprolactone: a review. Chemical Society Reviews. 2009;38(12):3484.

[35] Thomas S, DiCosimo R, Nagarajan V. Biocatalysis: applications and potentials for the chemical industry. Trends in Biotechnology. 2002;20(6):238-242.

[36] Braud C, Devarieux R, Atlan A, Ducos C, Michel Vert. Capillary zone electrophoresis in normal or reverse polarity separation modes for the analysis of hydroxy acid oligomers in neutral phosphate buffer. Journal of Chromatography B: Biomedical Sciences and Applications. 1998;706(1):73-82.

[37] Khanna A, Sudha Y, Pillai S, Rath S. Molecular modeling studies of poly lactic acid initiation mechanisms. Journal of Molecular Modeling. 2008;14(5):367-374.

[38] Zhang Y, Wang D, Wurst K, Buchmeiser M. Ring-opening polymerization of cyclohexene oxide by a novel dicationic palladium catalyst. Designed Monomers and Polymers. 2005;8(6):571-588.

[39] Kim M, Seo K, Khang G, Lee H. Ring-Opening Polymerization of?-Caprolactone by Poly(ethylene glycol) by an Activated Monomer Mechanism. Macromolecular Rapid Communications. 2005;26(8):643-648.

[40] Vert M, Li S, Spenlehauer G, Guerin P. Bioresorbability and biocompatibility of aliphatic polyesters. Journal of Materials Science: Materials in Medicine. 1992;3(6):432-446.
[41] Vert M. Degradable and bioresorbable polymers in surgery and in pharmacology: beliefs and facts. Journal of Materials Science: Materials in Medicine. 2008;20(2):437-446.
[42] Deng Y, Yang L. Preparation and characterization of polyethylene glycol (PEG) hydrogel as shape-stabilized phase change material. Applied Thermal Engineering. 2017; 114:1014-1017.
[43] Sarı A. Composites of polyethylene glycol (PEG600) with gypsum and natural clay as new kinds of building PCMs for low temperature-thermal energy storage. Energy and Buildings. 2014;69:184-192.
[44] Hesse E, Hefferan T, Tarara J, Haasper C, Meller R, Krettek C et al. Collagen type I hydrogel allows migration, proliferation, and osteogenic differentiation of rat bone marrow stromal cells. Journal of Biomedical Materials Research Part A. 2010;94:442–449.
[45] Prestwich G, Kuo J. Chemically-Modified HA for Therapy and Regenerative Medicine. Current Pharmaceutical Biotechnology. 2008;9(4):242-245.
[46] Gilsenan P. Rheological characterisation of gelatins from mammalian and marine sources. Food Hydrocolloids. 2000;14(3):191-195.
[47] Utech S, Boccaccini A. A review of hydrogel-based composites for biomedical applications: enhancement of hydrogel properties by addition of rigid inorganic fillers. Journal of Materials Science. 2015;51(1):271-310.
[48] Biswal D, Anupriya B, Uvanesh K, Anis A, Banerjee I, Pal K. Effect of mechanical and electrical behavior of gelatin hydrogels on drug release and cell proliferation. Journal of the Mechanical Behavior of Biomedical Materials. 2016;53:174-186.
[49] Sarker B, Papageorgiou D, Silva R, Zehnder T, Gul-E-Noor F, Bertmer M et al. Fabrication of alginate–gelatin crosslinked hydrogel microcapsules and evaluation of the microstructure and physico-chemical properties. Journal of Materials Chemistry B. 2014;2(11):1470.
[50] Dainiak M, Allan I, Savina I, Cornelio L, James E, James S et al. Gelatin–fibrinogen cryogel dermal matrices for wound repair: Preparation, optimisation and in vitro study. Biomaterials. 2010;31(1):67-76.
[51] URTTI A. Biomaterials for RPE tissue engineering and cell microencapsulation. Acta Ophthalmologica. 2009;87:65-68.
[52] Ahmed T, Dare E, Hincke M. Fibrin: A Versatile Scaffold for Tissue Engineering Applications. Tissue Engineering Part B: Reviews. 2008;14: 199–215.

[53] Fedorovich N, Alblas J, de Wijn J, Hennink W, Verbout A, Dhert W. Hydrogels as Extracellular Matrices for Skeletal Tissue Engineering: State-of-the-Art and Novel Application in Organ Printing. Tissue Engineering. 2007;13(8):1905-1925.

[54] Drury JL, Mooney DJ. Hydrogels for tissue engineering: scaffold design variables and applications. Biomaterials 2003;24(24):4337–51

[55] Murphy SV, Skardal A, Atala A. Evaluation of hydrogels for bioprinting applications. J Biomed Mater Res Part A 2013;101(1):272–84.

[56] Chang C, Boland E, Williams S, Hoying J. Direct-write bioprinting three-dimensional biohybrid systems for future regenerative therapies. Journal of Biomedical Materials Research Part B: Applied Biomaterials. 2011;98B(1):160-170.

[57] Guillotin B, Guillemot F. Cell patterning technologies for organotypic tissue fabrication. Trends in Biotechnology. 2011;29(4):183-190.

[58] Grigore A, Sarker B, Fabry B, Boccaccini A, Detsch R. Behavior of Encapsulated MG-63 Cells in RGD and Gelatine-Modified Alginate Hydrogels. Tissue Engineering Part A. 2014;20(15-16):2140-2150.

[59] Boanini E, Rubini K, Panzavolta S, Bigi A. Chemico-physical characterization of gelatin films modified with oxidized alginate. Acta Biomaterialia. 2010;6(2):383-388.

[60] Ivanovska J, Zehnder T, Lennert P, Sarker B, Boccaccini A, Hartmann A et al. Biofabrication of 3D Alginate-Based Hydrogel for Cancer Research: Comparison of Cell Spreading, Viability, and Adhesion Characteristics of Colorectal HCT116 Tumor Cells. Tissue Engineering Part C: Methods. 2016;22(7):708-715.

[61] Detsch R, Sarker B, Zehnder T, Frank G, Boccaccini A. Advanced alginate-based hydrogels. Materials Today. 2015;18(10):590-591.

[62] Jung J, Lee H, Hong J, Park J, Shim J, Choi T et al. A new method of fabricating a blend scaffold using an indirect three-dimensional printing technique. Biofabrication. 2015;7(4):045003.

[63] Gong C, Shi S, Dong P, Kan B, Gou M, Wang X et al. Synthesis and characterization of PEG-PCL-PEG thermosensitive hydrogel. International Journal of Pharmaceutics. 2009;365(1-2):89-99.

[64] Sigma Aldrich, "Polycaprolactone average Mn 45,000," 2. [Internet]. [Cited 2018 Mar 1]. Available from: http://www.sigmaaldrich.com/catalog/product/aldrich/704105?lang=de®ion=DE.

[65] GeSiM mbH, “BioScaffolder 3.1,” 2016. [Internet].[Cited 2018 Mar 1]. Available from: https://gesim-bioinstrumentsmicrofluidics.com/wp-content/uploads/2016/04/GESIM- BS31_web_0416.pdf.

INFORMATION FOR LIBRARY DATABASE

Title	3D bioprinting using hydrogel and synthetic fillers
Author	Niloufar Rashedi Banafshehvaragh
Year of defence	2018
Supervisor	doc. Ing. Petr Němec, Ph.D.
Annotation	The aim of this research is to make a comparison between pure polycaprolactone (PCL) and a combination of polycaprolactone and polyethylene glycol (PCL-PEG) blend together with alginate dialdehyde gelatin hydrogel (ADA-GEL) to fabricate 3D scaffolds with sequential bioprinting process.
Keywords	3D bioprinting; additive manufacturing technique; biofabrication; tissue engineering; polycaprolactone; alginate dialdehyde gelatin; hydrogels